

Review

A Review of the Application of Hemispherical Photography in Urban Outdoor Thermal Comfort Studies

Lei Sima ^{1,*}, Yisha Liu ^{1,*}, Xiaowei Shang ^{2,*}, Qi Yuan ² and Yunming Zhang ¹

¹ Department of Architecture, College of Architecture and Urban Planning, Tongji University, Siping Campus, Shanghai 200092, China

² School of Civil Engineering and Architecture, Southwest University of Science and Technology, Mianyang 621051, China

* Correspondence: sima@tongji.edu.cn (L.S.); 2410318@tongji.edu.cn (Y.L.); sxwarchitect@swust.edu.cn (X.S.)

Abstract: Thermal comfort studies are paramount in enhancing future urban living conditions, and hemispherical photography has emerged as a widely employed field measurement technique in outdoor thermal comfort research. This comprehensive review systematically analyzed 142 outdoor thermal comfort studies conducted over the past decade using hemispherical photography methods, revealing that its primary application lies in objectively describing environmental information and constructing associated indices. In contrast, the number of studies focusing on subjectively assessing environmental factors remains relatively low; however, it is rapidly increasing due to its demonstrated effectiveness and convenience compared to other methodologies within this domain. Overall, despite certain limitations, such as higher labor costs and limited temporal/spatial coverage when describing environmental information, hemispherical photography still retains its advantage of providing accurate data acquisition for outdoor thermal comfort research. In recent years, advancements in mobile measurement tools and techniques have enhanced the richness and versatility of acquired information while leveraging the image specificity inherent to hemispherical photography, which continues to play a pivotal role in subjective assessments related to human perception of outdoor thermal comfort.

Keywords: hemispherical photography; outdoor thermal comfort; environmental information; fisheye lens



Academic Editor: Antonio Caggiano

Received: 30 November 2024

Revised: 29 December 2024

Accepted: 31 December 2024

Published: 2 January 2025

Citation: Sima, L.; Liu, Y.; Shang, X.; Yuan, Q.; Zhang, Y. A Review of the Application of Hemispherical Photography in Urban Outdoor Thermal Comfort Studies. *Buildings* **2025**, *15*, 123. <https://doi.org/10.3390/buildings15010123>

Copyright: © 2025 by the authors. Licensee MDPI, Basel, Switzerland. This article is an open access article distributed under the terms and conditions of the Creative Commons Attribution (CC BY) license (<https://creativecommons.org/licenses/by/4.0/>).

1. Introduction

In 2007, for the first time, the number of people living in urban areas surpassed those in rural regions [1], with more than 50 percent of the world's population living in cities [2], and urban outdoor spaces hosting most of the daily lives of their inhabitants. However, due to changes in the surface structure of the city, natural and green surfaces have been replaced by roads and impervious surfaces, which has reduced the OTC (outdoor thermal comfort) and weakened the livability of the city [3]; therefore, improving the OTC of the city has become more and more important in urban development to guarantee the quality of life of the city's inhabitants [4].

Thermal comfort, defined as “the psychological state of being satisfied with the thermal environment”, has been extensively studied and standardized, considering both physical and physiological factors and psychological influences [5]. Numerous models have been developed to assess thermal comfort, including the PMV (Predicted Mean Vote) model introduced by Fanger in the late 1960s, which has since become a cornerstone in thermal comfort research [6], and thermal comfort is essential for everyone to have a healthy and

efficient lifestyle [7]. In the past, thermal comfort studies were generally conducted only indoors until the beginning of the 21st century, when thermal comfort in urban outdoor environments gradually received attention [8]. The thermal environment can be described as the environmental characteristics affecting the heat exchange between the human body and the environment [9]. The environmental factors affecting human thermal comfort in outdoor environments are complex. They can usually be categorized into physical environmental factors [10] (based on the consideration of the balance between heat production and heat dissipation) and non-physical environmental factors [11] (personal, social, and psychological factors, etc.). Scholars currently use both subjective and objective methods to research urban OTC. The subjective approach focuses on the actual thermal perception of people in a specific outdoor environment and mainly uses qualitative methods such as interviews and questionnaires. On the other hand, objective methods use quantitative measurements to assess the energy interactions between the human body and the surrounding environment. Environmental information is generally obtained through various experimental instruments [12].

Researchers have created many methods for thermal comfort studies, usually categorized as field measurements, simulation studies, remotely sensed imagery, weather station studies, etc. [13]. Among them, remote sensing is a technique that employs sensors mounted on satellites or aircraft to collect surface data. It can acquire continuous large-scale information on subsurface structures and surface temperatures [14]. However, the resolution of satellite-based remote sensing is constrained by payload capacity and sensor technology limitations, making it challenging to capture detailed surface features. Therefore, remote sensing is frequently employed for urban-wide studies. The temporal resolution of remote sensing data is typically coarser, with the observation interval for Landsat 8 satellite data being 16 days [15]. In contrast, hemispherical photography is an in situ measurement technique that captures more immediate, detailed, and realistic environmental information. Consequently, it is extensively utilized in OTC research and represents a well-established method.

In the early stages, hemispherical photography for acquiring environmental information was predominantly conducted at fixed points using wide-angle lenses [16]. Subsequently, this method has been integrated with various advanced technologies, including infrared detection [17], LiDAR [18], Google Street View [19], drones [4], and simulation software [20].

As a special image method, hemispherical photography has been deeply involved in various types of OTC studies. Ahmadi Venhari et al. utilized hemispherical photography to compare the cooling effects of different plant types, demonstrating that not all plants provide equivalent cooling benefits, with trees offering the most significant cooling effect through shading [10]. Sharmin et al. employed a plant canopy analyzer to capture hemispherical images of trees in Australia and discovered that temperature variations were influenced by Leaf Area Index (LAI) and canopy width, with each unit increase in LAI resulting in a 1.1 °C decrease in temperature [21]. Chàfer et al. found that urban land use models constructed using hemispherical cameras exhibited a strong correlation with temperature changes in Singapore [22].

However, previous studies usually only regard hemispherical photography as an image-based intermediate result [23] and do not consider it as a relatively independent research method and tool for systematic investigation. The application of hemispherical photography in previous studies has been somewhat random, failing to fully leverage its advantages for more purposeful use by researchers. To address this issue and enhance the rationality of hemispherical photography applications in future research, this study selects hemispherical photography as the research object. By summarizing the utilization

of hemispherical photography in OTC research over the past decade, this study explores the transformation of its application, aims to summarize its characteristics and future development trends, and seeks to provide a clearer and more reasonable methodology for researchers who apply hemispherical photography in OTC research.

2. Literature Screening and Data Description

2.1. Literature Screening

This study conducted a systematic literature review using the PRISMA (Preferred Reporting Items for Systematic Reviews and Meta-Analyses) framework [24]. The selected literature was restricted to studies of urban OTC utilizing hemispheric photography methods. Specifically, this means that the study sites need to be within cities, including central business districts, city squares, city parks, commercial areas, street canyons, residential neighborhoods, schools, courtyards, waterfront spaces, and industrial zones. The research methodology explicitly involves the use of hemispherical photography to gather environmental data, which serves as raw material for constructing relevant environmental information indicators. This includes references to the application of hemispherical photographic tools in the text or the direct presentation of hemispherical photographic images in accompanying figures. The time frame for the study is restricted to the past decade, i.e., relevant literature from 2015 to 2024 was retrieved from the Web of Science and Scopus databases.

During the literature search, the relevant literature was searched using the terms “hemisphere photography”, “fisheye lens”, “outdoor thermal comfort”, “outdoor thermal comfort index”, “heat stress”, “urban heat island”, “outdoor environment”, and “human thermal comfort”. The keywords were linked together using the Boolean operators “AND” and “OR” to obtain the most relevant literature.

The literature search yielded a total of 620 relevant papers, with 173 duplicates removed through manual search. Subsequently, the remaining 447 papers were screened based on the following criteria: (1) papers not in English were excluded; (2) studies without the use of hemispherical photography were excluded; (3) studies not related to thermal comfort research were excluded; (4) studies only focused on indoor thermal comfort were excluded; (5) review studies were excluded.

Based on the above criteria, 142 papers were retained for analysis. Figure 1 shows the flowchart of the literature search and screening process following the PRISMA statement.

2.2. Data Description

This section provides a comprehensive summary of the journal sources of the available studies, the distribution of study areas, climatic conditions, seasons and weather patterns, the selection criteria for study sites, and the primary objectives of the studies. The analysis of the 142 studies reveals that OTC studies utilizing hemispheric photography are predominantly concentrated in Asia, especially in developed countries and regions in the mid-latitudes of the Northern Hemisphere, with climate subdivisions dominated by Cfa, Cwa, Cfb, and Dwa. The studies predominantly concentrate on summer heat stress, particularly under sunny conditions, with street canyons serving as the most frequent study sites. The core research objectives revolve around cooling mechanisms and the optimization of urban spaces.

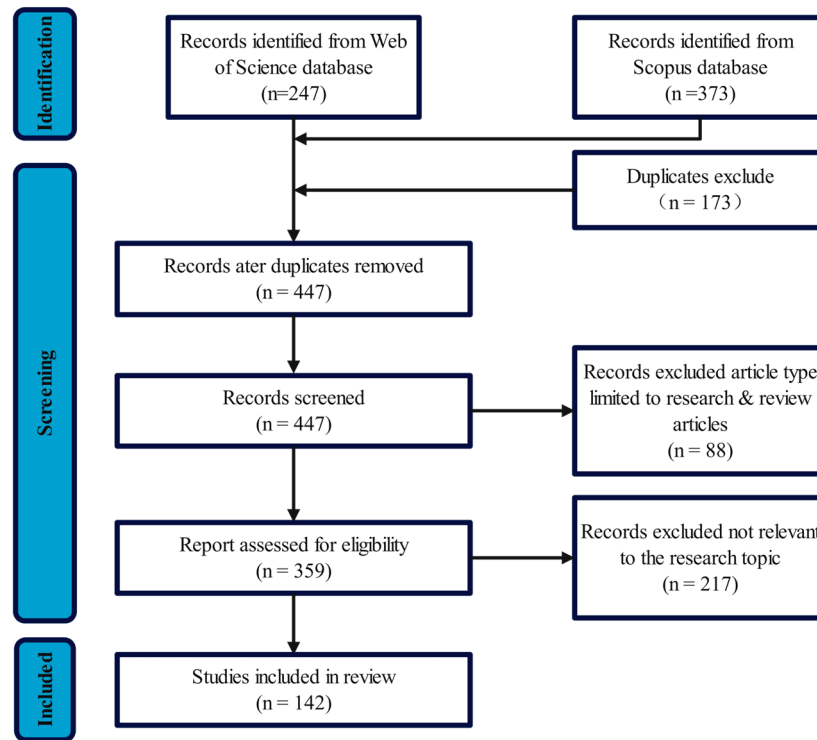


Figure 1. Flowchart for literature search and screening following the PRISMA statement.

2.2.1. Literature Information

A total of 142 papers met the selection criteria and were included in the analysis. Figure 2 shows the journal source information of the papers, among which “Building and Environment” is the journal with the most papers published in this field, with a total of 42 papers; “Sustainable Cities and Society”, “Urban Climate”, “Urban Forestry & Urban Greening”, and “Science of The Total Environment” also have more than 10 papers.

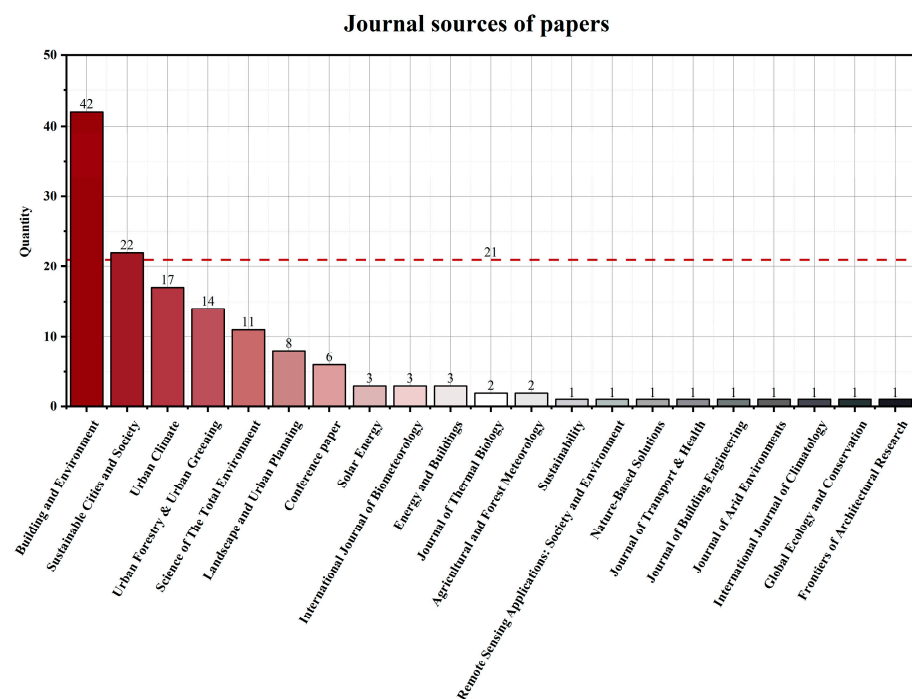


Figure 2. Journal sources of papers.

Figure 3 illustrates the regional distribution of research, with statistics limited to regions where primary research sites are located for standardization purposes. Asia is the most extensively studied region, accounting for over 60% of all studies, followed by Europe at just over 14%. Research areas are concentrated in mid-latitude regions of the Northern Hemisphere, primarily in developed countries and those experiencing rapid economic growth. Figure 4 shows the Köppen–Geiger classification for all studies, with Cfa, Cwa, Cfb, and Dwa being the most researched climate divisions, with a combined share of more than 64%.

Geographical location

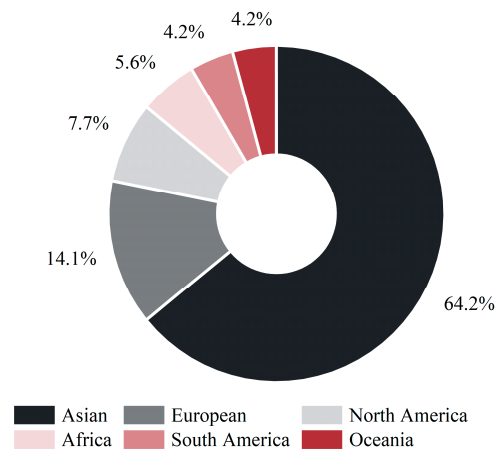


Figure 3. Percentage of geographical locations.

Köppen climate classification

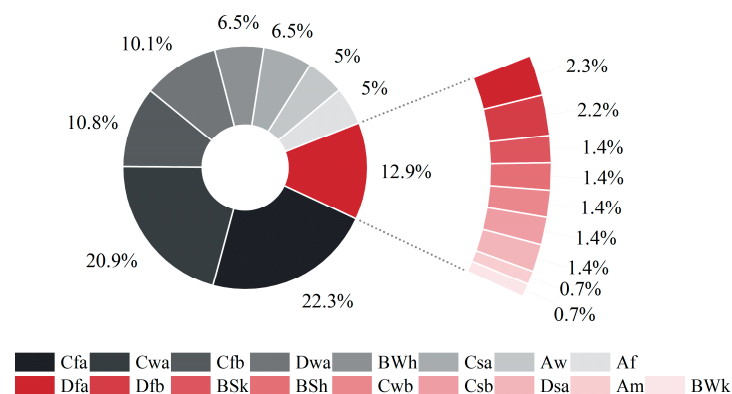


Figure 4. Percentage of Köppen Climate Classification.

2.2.2. Description of Research Content

The 142 papers exhibit distinct variations in seasonal and climatic distributions (Figure 5), with summer being the predominant focus for investigating significant heat stress (72% of studies conducted research during this season). Similarly, winter received more attention as a period associated with severe heat discomfort (21% of studies conducted research during this season), and 76% of studies conducted in winter also encompassed investigations during summer. Regarding climate, studies on tropical climates were notably limited, accounting for only 2% of all research endeavors. Additionally, 15% of the studies employed modeling techniques without addressing particular seasons and climates.

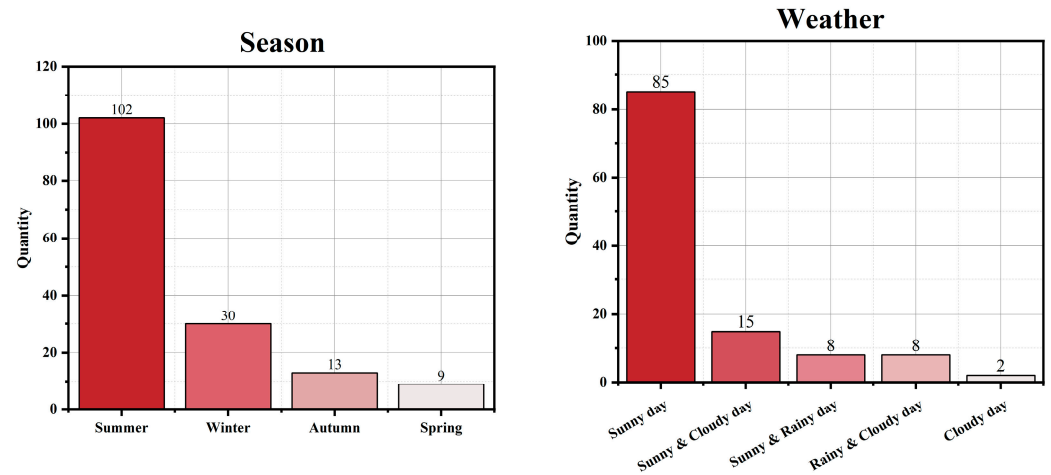


Figure 5. Conducting frequencies of various weather and seasons.

Furthermore, variations were observed in the conducted studies about different weather conditions (Figure 5), with certain studies failing to specify the weather conditions under investigation. Among those that did provide details on weather conditions, a majority of 83% solely focused on sunny conditions. Only 17% of the studies considered cloudy conditions, while 8% accounted for rainy and snowy conditions, and these studies often choose to compare their findings against those obtained under sunny conditions.

Figure 6 depicts the distribution of research locations selected for statistical papers. Street canyons emerge as the predominant choice among researchers (34%). Furthermore, city parks (25%), schools (22%), residential neighborhoods (13%), and city squares (11%) were also extensively favored by researchers.

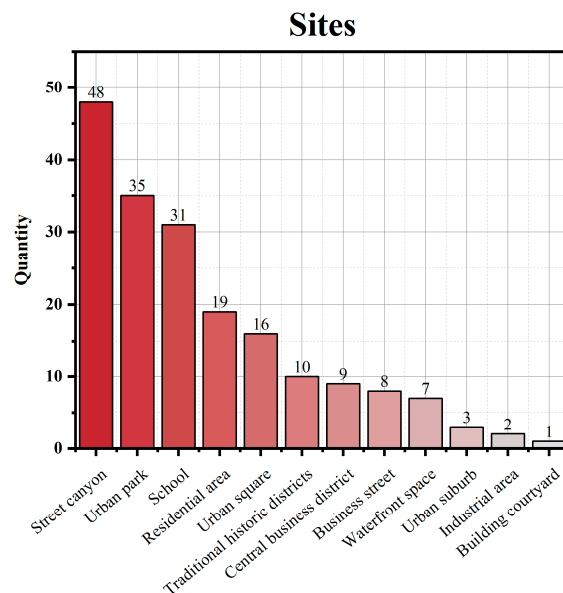


Figure 6. Conducting frequencies of surveying sites.

Figure 7 illustrates the distribution of the number of study sites. Due to limitations in the spatial and temporal spans of field measurements, 62% of the studies opted for fewer than 20 sites. However, with the rapid emergence of mobile measurements, more than 23% of the studies have shifted away from a limited number of fixed sites and now prefer obtaining continuous environmental information through mobile measurements.

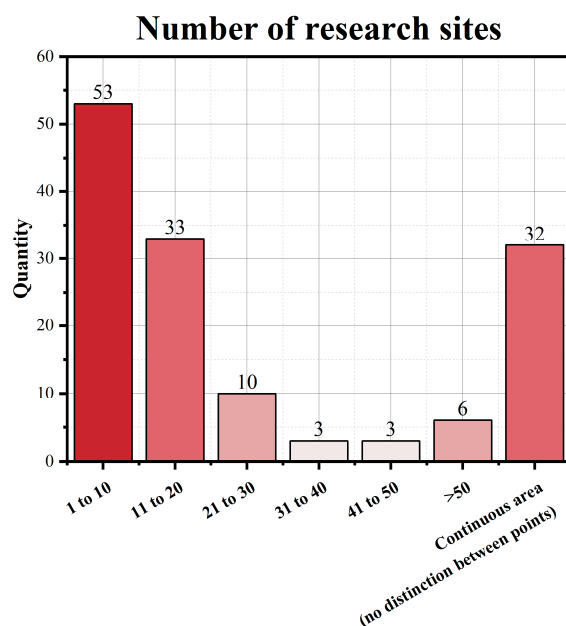


Figure 7. Percentage of the number of research sites.

Figure 8 shows the frequencies of the study periods, highlighting midday to afternoon as the predominant period for thermal discomfort investigation (73%). Over 40% of the studies opted for a full day as their study duration to obtain a more comprehensive understanding of thermal comfort trends. Due to the cost and difficulty associated with field measurements, simulation-based approaches have gained popularity in these extended-duration investigations since 2023 (Figure 9).

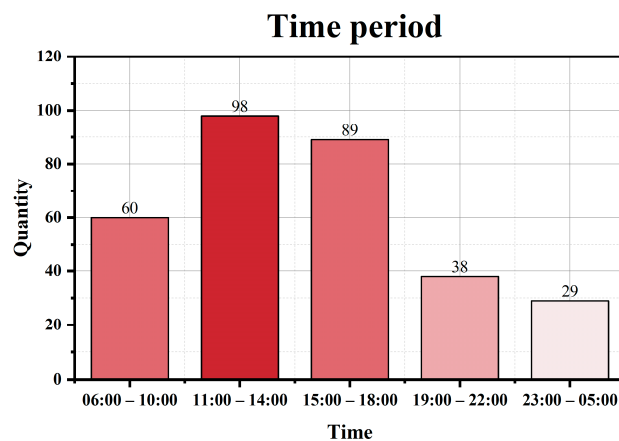


Figure 8. Frequencies of the study periods.

The distribution of research objectives for all papers is illustrated in Figure 10, where the dominant research objectives are cooling mechanisms and urban spatial optimization strategies (88%). Although many studies focused on a single research objective, more than 17% researched multiple objectives simultaneously. Furthermore, while only a limited number of studies have aimed at research method optimization, the share of studies with this aim has gradually increased in recent years.

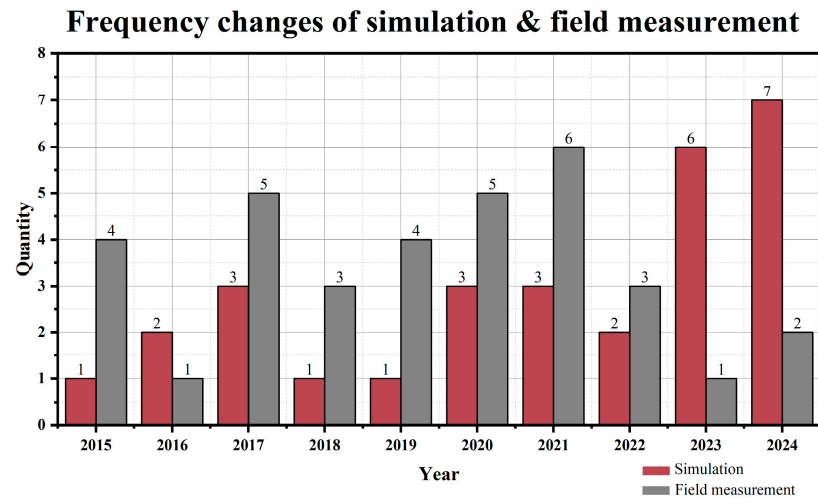


Figure 9. Trends in different methods of obtaining one-day data.

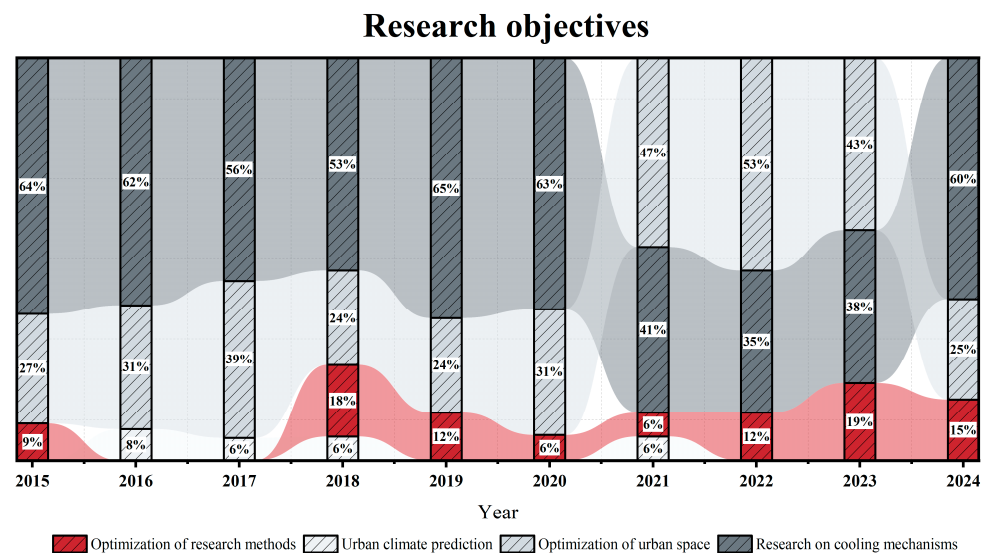


Figure 10. Trends in research objectives.

3. Hemispherical Photography Construction Method in OTC

Various image acquisition tools have been utilized for hemispherical photography in different studies, including a fisheye lens, plant canopy analyzer, Street View images, infrared detection technology, LiDAR, Mobile Measuring Platform, and simulation. Each tool possesses distinct characteristics, and the specific methods for constructing hemispherical photographs using these tools are described below.

3.1. Fisheye Lens

A fisheye lens is a specialized ultra-wide-angle photographic lens, typically with a focal length of 16 mm or less, that offers an angle of view close to or even exceeding 180 degrees and can capture a scene comparable to or wider than the human eye's visual range [25] (Table 1). The resulting photographs exhibit "barrel distortion", causing straight lines to curve at the image edges [26] (Figure 11). In the field of OTC research, hemispherical photography utilizing a fisheye lens represents the oldest method employed. Typically, this technique involves mounting a DSLR camera horizontally on a tripod with a fisheye lens set at 180 degrees and capturing images of the sky [27]. Some studies opt for vertically photographing the ground at 90 degrees [28] (Figure 12). This construction method stands

as the most widely accepted approach in hemispherical photography due to its proven accuracy and validity within OTC studies [29].

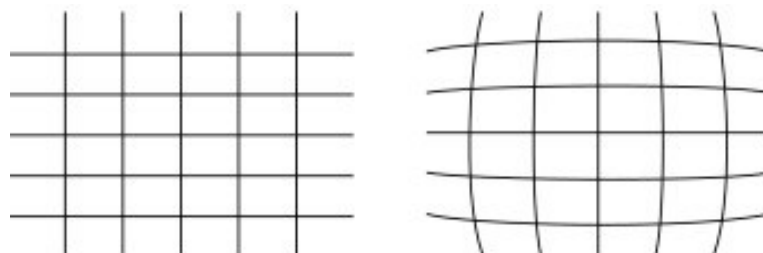


Figure 11. Barrel distortion effect of a rectangular grid [26].

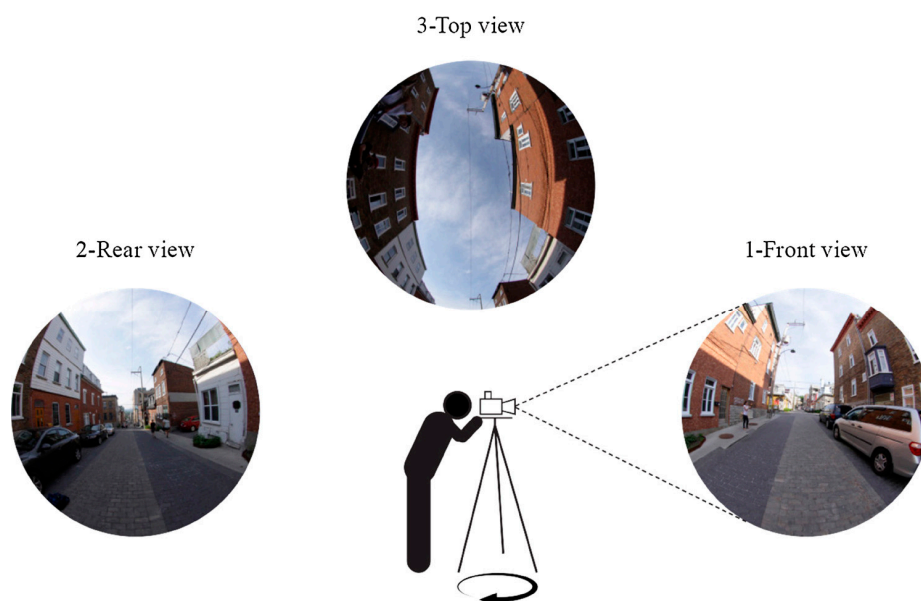


Figure 12. Hemisphere photography with a fisheye lens [28].

In recent years, to utilize the unique spectral response properties of photosynthetically active plant elements [30], researchers used the Blue IR filter (a filter introduced by Kolari Vision that transmits both blue light and infrared light for NDVI crop analysis applications) to replace the camera's hot mirror to take dual-wavelength hemispherical photography to achieve effective acquisition of richer environmental information [31] (Figure 13). In general, the use of a fisheye lens to acquire hemispherical photography is more costly in terms of time and labor and usually can only obtain a small amount of fixed-point environmental information, which does not apply to the acquisition and description of composite information in a wide range of space [32].

Table 1. Summary of fisheye lens.

| Model | Image | Manufacturer | Brief Introduction | Features | Literature |
|-------|---|---------------------|---|---|------------|
| FC-E8 |  | NIKON, Tokyo, Japan | 10.5 mm fixed focal length, maximum aperture of $f/2.8$, designed for DX-format cameras. | Lightweight, low price, average low-light imaging quality. | [16,33–35] |
| FC-E9 |  | NIKON, Tokyo, Japan | 10.5 mm fixed focal length, maximum aperture of $f/2.8$, designed for DX-format cameras. | Improved model of the FC-E8, with improved image quality, lightweight, and low price. | [36] |

Table 1. Cont.

| Model | Image | Manufacturer | Brief Introduction | Features | Literature |
|---|---|-----------------------------------|---|--|------------|
| AF DX Fisheye-Nikkor 10.5 mm f/2.8G ED |  | NIKON, Tokyo, Japan | 10.5 mm fixed focal length with a maximum aperture of f/2.8 for APS-C cameras. | High image quality, large aperture, good imaging effect in low light environment, high price, no zoom function. | [37] |
| AF-S Fisheye NIKKOR 8–15 mm f/3.5–4.5E ED |  | NIKON, Tokyo, Japan | 8–15 mm focal length range and f/3.5–4.5 maximum aperture, supports both full-frame (FX format) and APS-C (DX format) sensors. | Highly versatile, uses Nikon ED lens technology to effectively reduce glare and dispersion, and has excellent image quality. Expensive, small aperture, and low-light performance is not as good as f/2.8 lens. It is heavy and not easy to carry. | [38,39] |
| T197412 |  | FLIR, Portland, OR, USA | Thermal imaging fisheye lens with fixed aperture range for FLIR's infrared thermal imaging devices only. | Non-traditional photographic lens, cannot be used for visible light photography, less versatile, imaging resolution dependent on infrared equipment, low accuracy. | [40] |
| 4.5 mm f 2.8 EX |  | SIGMA, Kanagawa, Japan | Diagonal fisheye lens with a fixed focal length of 4.5 mm and a maximum aperture of f/2.8 for APS-C cameras. | This lens is designed for APS-C, has high image quality, is compact and lightweight, and is cost-effective, but does not support zoom. | [31,41–44] |
| 8 mm F3.5 EX DG |  | SIGMA, Kanagawa, Japan | Round fisheye lens with an ultra-wide focal length of 8 mm and a maximum aperture of F3.5 for full-frame cameras. | Optical quality is good, with reasonable chromatic aberration and flare control, but with an aperture of f/3.5 and mediocre low-light capabilities, it is a cost-effective lens for full-frame cameras. | [18,45–49] |
| EF 8–15 mm f/4L Fisheye USM |  | CANON, Tokyo, Japan | Zoom fisheye lens with 8–15 mm focal length range and f/4 maximum aperture for full-frame, APS-C cameras. | Supports zoom from circular fisheye (8 mm) to diagonal fisheye (15 mm) with very high optical quality, but with a maximum aperture of f/4, it does not perform as well as the f/2.8 lens in low light, and it is expensive and heavy. | [41,50–53] |
| SL-FE12 |  | SUMLUNG, Shanghai, China | Quick-detachable fisheye lens designed for smartphones. | Low image quality, but extremely portable and far less expensive than comparable brands. | [54] |
| Oloclip fisheye converter |  | OLLOCLIP, Foothill Ranch, CA, USA | A portable lens set designed for smartphones, the 3-in-1 Lens Kit Includes Fisheye, Super-Wide, and Macro 15x Premium Glass Lenses. | Imaging quality is limited, not comparable to professional camera lenses, only available for some cell phone models, and less versatile. | [55] |
| NDVI Blue IR filter ZB2 |  | KOLARI, Raritan, NJ, USA | KOLARI's filter can transmit both blue light and infrared light. | It is very suitable for NDVI crop analysis applications. | [31] |

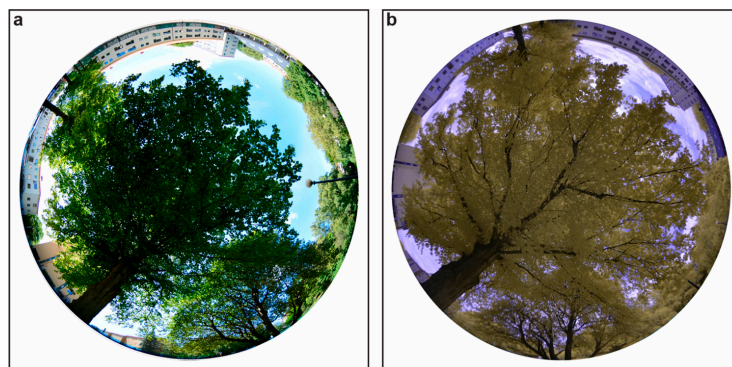


Figure 13. Dual-wavelength photographs were taken at the same location ((a) is the original picture, and in (b), the leaves were yellow due to the existence of a filter) [31].

3.2. Plant Canopy Analyzer

The plant canopy analyzer is an instrument utilized to investigate plant canopy structure and growth (Table 2). It serves as an effective tool to acquire information regarding the location, size, density, and distribution of gaps within the plant canopy [56]. Equipped with a fisheye lens and an optical system comprising five concentric ring detectors (Figure 14), its latest enhanced model, “LAI-2200C”, enables precise measurements under diverse sky conditions without necessitating specific sun angles or cloud cover conditions [57]. Although similar to hemispherical photography obtained through a fisheye lens, the plant canopy analyzer surpasses it in terms of automated data processing capabilities while minimizing errors associated with camera positioning, exposure, and skylight uniformity; however, this comprehensive system also entails higher costs.

Table 2. Summary of plant canopy analyzer.

| Model | Image | Manufacturer | Brief Introduction | Features | Literature |
|----------|---|---------------------------|--|--|---------------|
| LAI-2200 |  | LI-COR, Lincoln, NE, USA | It is an upgraded product of LAI-2000, which is equipped with an FV2200 software program to measure plant canopy information through optical multi-angle, non-destructive. | Compared with LAI-2000, it has a new Radiation Shield with higher accuracy and compatibility, wide applicability, data that can be used directly for canopy modeling and photosynthetic efficiency research, and more advanced software and data processing functions. However, it is expensive. | [18,21,31,58] |
| LAI-2000 |  | LI-COR, Lincoln, NE, USA | It can measure plant canopy information optically from multiple angles and non-destructively; it is based on blue light band (320–490 nm) measurement to minimize spectral interference. | It provides stable measurements and is suitable for large-scale ecosystem studies. It is not suitable for highly scattered light environments. The software has limited processing power and requires additional tools for data analysis. Lower cost than LAI-2200. | [59,60] |
| HemiView |  | DYNAMAX, Houston, TX, USA | It measures plant canopy information based on fisheye photographic images, which are intuitive and flexible for a variety of environments. | Low cost, intuitive results (canopy structure can be observed directly through the image). Flexible operation and rich post-processing functions, but the measurement results are easily affected by light conditions, and the analysis accuracy is limited by image resolution and processing algorithms. | [61] |

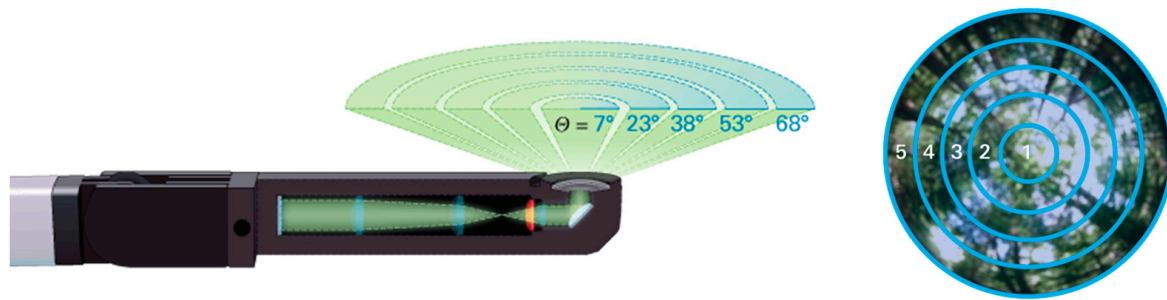


Figure 14. LAI-2200C Plant canopy analyzer optical sensor with 5 concentric ring detectors schematically shown on the **left** and hemispherical photography acquired by it on the **right** [57].

3.3. Street View Images

Street View images are panoramic photographs taken at a height of approximately 2.5 m from street level, incorporating location information and presented as interactive VR photos through stitching techniques [62]. This service was initially launched by Google Inc., the pioneering mapping service provider, in the United States in 2007. As of 2017, Google Inc. reported that their Street View coverage extended to over 83 countries worldwide [63]. Other companies such as Microsoft, Baidu, and Tencent also offer similar photo services (the latter two providing services primarily in China) [64]. Furthermore, there is a rapid growth in crowdsourcing Street View platforms maintained by regular users, exemplified by Mapillary and OpenStreetCam [65].

Given its ability to capture the vertical dimension of urban streetscapes and provide detailed information at a micro level, Street View images offer an environmental assessment that closely aligns with human perception [66,67]. In 2015, Carrasco-Hernandez et al. introduced the use of open-source software Hugin to project Google Street View onto a plane for constructing hemispherical photography [68]. Building upon this, Li et al. proposed a method in 2017 to convert Street View images from isometric cylindrical projection to isometric azimuthal projection for creating hemispherical photography, which has since been widely adopted in subsequent studies [19] (Figure 15). Due to its cost-effectiveness and extensive coverage across temporal and spatial scales, the utilization of street view imagery has increasingly become an important tool for investigating OTC in recent years [69]. Wang et al. [70] analyzed the spatial and temporal distribution of solar radiation from various directions in Beijing during summer using 100,000 Street View images, leveraging the low-cost advantage of this approach. Additionally, advancements in computer science have enabled more sophisticated extraction of hidden features from Street View images. For instance, transformer-based deep learning methods have been developed to detect obstacles in urban environments [71]. However, it should be noted that street view imagery suffers from infrequent updates and ambiguous update dates provided by map service providers. Additionally, its coverage is limited primarily to major vehicular streets with minimal representation in developing countries and rural areas.

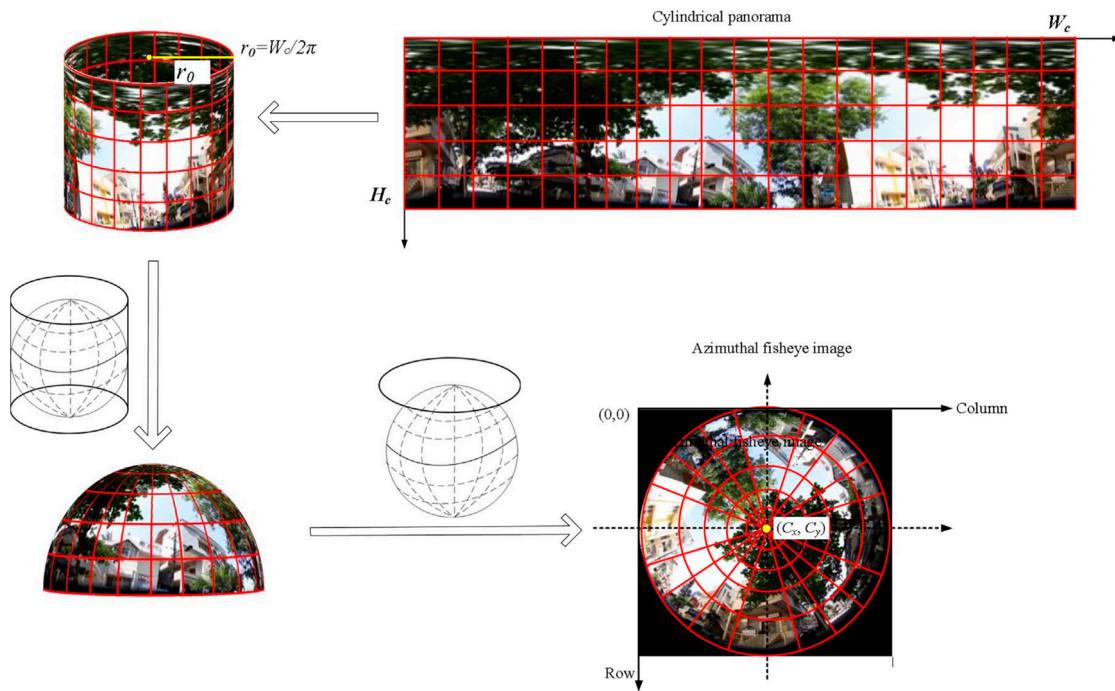


Figure 15. Schematic of the process of converting a Google Street View panorama from an isometric cylindrical projection to an isometric azimuthal projection [19].

3.4. Infrared Detection Technology

The images obtained through infrared detection techniques are commonly known as thermograms. This technique captures and visualizes the infrared radiant energy emitted by an object [28] (Table 3). In investigations of urban outdoor thermal environments, the radiative environment plays a crucial role in determining comfort levels [72]. In 2023, Middel et al. presented a thermographic panorama using a six-way hemispherical photography approach and constructed a hemispherical photograph utilizing the PanoMRT (Panoramic infrared thermography) model [17] (Figure 16). Due to its non-contact nature, thermal imaging is well-suited for assessing the micro-scale radiation environment in panoramic view mode. Merchant et al. [73] developed a camera system that records 360° shortwave and longwave panoramic images to address spatial variations in shortwave and longwave radiative heat transfer in outdoor environments. As a form of hemispherical photography that integrates multiple environmental information, infrared detection technology offers advantages such as reduced time consumption, high information density, and enhanced data accuracy when studying urban outdoor thermal radiation environments.

Table 3. Summary of infrared detection equipment.

| Model | Image | Manufacturer | Accuracy | Features | Literature |
|-------|---|-------------------------|--|---|------------|
| B50 |  | FLIR, Portland, OR, USA | Infrared resolution: 140 × 140; Measuring range: −20 °C to +120 °C; Thermal sensitivity < 0.1 °C | Portable thermal imaging camera, lightweight, affordable, lightweight, easy to carry, low resolution, suitable for primary inspection applications, not suitable for high-temperature environments. | [28] |
| T460 |  | FLIR, Portland, OR, USA | Infrared resolution: 320 × 240; Temperature range: −20 °C to +1200 °C; Thermal sensitivity < 0.03 °C | High-performance thermal imager, high sensitivity and high resolution, rich functions, high price, slightly large size. | [40] |

Table 3. Cont.

| Model | Image | Manufacturer | Accuracy | Features | Literature |
|---|---|-------------------------------|---|--|------------|
| Duo Pro R HD Dual-Sensor Drone Thermal Camera |  | FLIR, Portland, OR, USA | Infrared resolution: 640×512 ; Temperature range: $-20\text{ }^{\circ}\text{C}$ to $+150\text{ }^{\circ}\text{C}$; Thermal sensitivity $< 0.05\text{ }^{\circ}\text{C}$ | Thermal imagers designed for drones, combining thermal imaging and HD visible camera functions, high resolution, support integration with drones, compatibility requirements for drone platforms, and higher prices. | [17] |
| Thermo FLEX F50 |  | Nippon Avionics, Tokyo, Japan | Infrared resolution: 240×180 ; Temperature range: $-10\text{ }^{\circ}\text{C}$ to $+400\text{ }^{\circ}\text{C}$; Thermal sensitivity $< 0.08\text{ }^{\circ}\text{C}$ | Portable thermal imager with easy rotation and separation of the camera head and controller, easy to operate, cost-effective, full-featured, low resolution, and average sensitivity. | [74] |

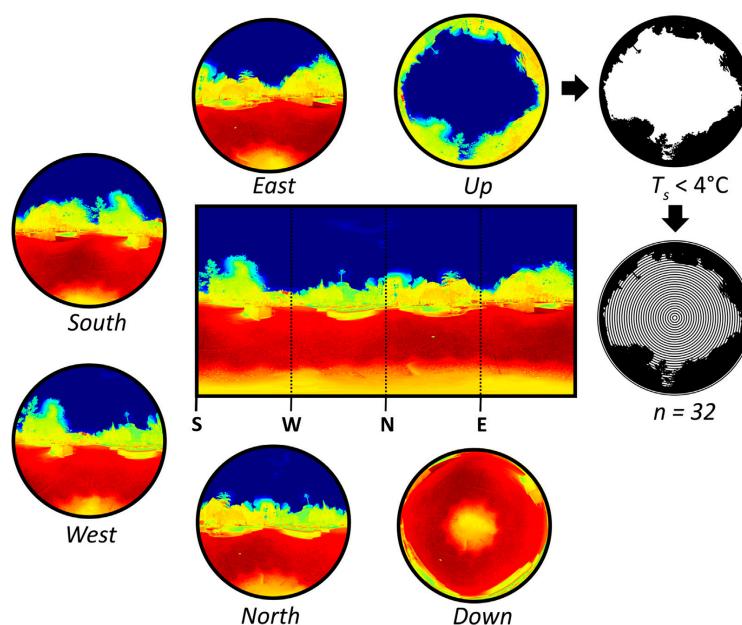


Figure 16. Thermal imaging panoramas projected as 6-way hemispherical photography [17].

3.5. LiDAR (Light Detection and Ranging)

In recent years, the utilization of TLS (Terrestrial laser scanning) equipment has witnessed a rapid surge in urban OTC studies due to the advancements in LiDAR-based technology [75]. High-precision TLS devices with a resolution range of 0.05–10 cm have proven to be effective in accurately characterizing vegetation structure and urban geometry [76], while their ability to acquire 3D point cloud data remains unaffected by time and weather constraints [77]. In these studies, GIS (geographic information system) processing of the obtained 3D point cloud information can facilitate the construction of hemispherical photography for calculating the canopy projection scale (Figure 17). The use of LiDAR technology for constructing hemispherical photography enables the acquisition of vegetation canopy information such as LAI (leaf area index) and SVF without being dependent on specific light environment conditions. This approach allows for precise quantification of the cooling effect resulting from vegetation shading and facilitates an assessment of localized solar radiation availability and cooling impact [18]. Despite its relatively high cost, LiDAR technology has demonstrated its accuracy advantage in characterizing vegetation canopy

morphology [18], urban geometric morphology [78], and radiation environment [79] when applied in OTC studies.

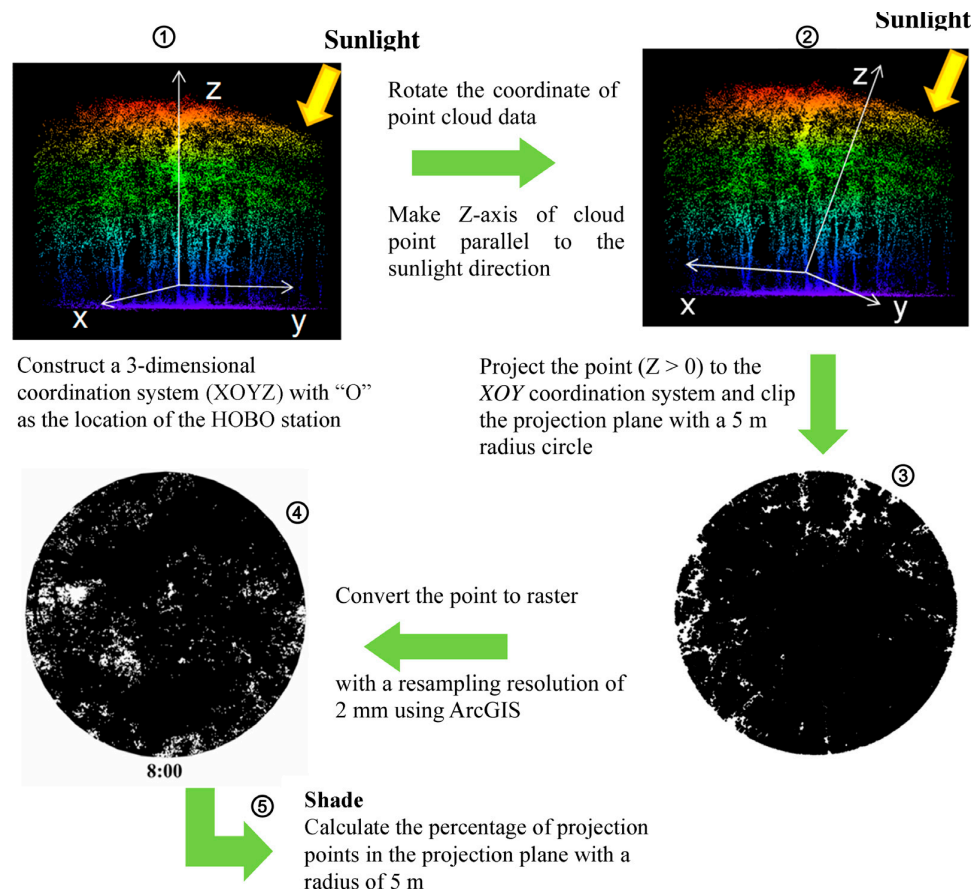


Figure 17. The 3DPC was processed to obtain the hemispherical projection using GIS software, and the scale of the canopy projection was calculated for a radius of 5 m [18].

3.6. Mobile Measuring Platform

Mobile surveying requires a range of mobile surveying platforms, including drones, unmanned vehicles, and homemade equipment delivery platforms. Among these options, drones are the most utilized tools for mobile measurement platforms. They can capture millimeter-resolution images by flying at low altitudes (~150 m) and can also achieve precise measurements of specific urban physical environments by utilizing different sensors [80]. The freedom and flexibility of drone flight enable data collection at various altitudes and locations, allowing for more comprehensive and accurate environmental information across the vertical gradient of the city [81]. In OTC studies, unmanned delivery platforms represented by drones serve as high-performance carriers equipped with high-resolution cameras [4], spectral sensors [82], LiDAR sensors [83], and temperature and humidity sensors [81]. These capabilities facilitate the acquisition of environmental data to construct hemispherical photography.

Street View images can serve as a passive mobile measurement method in outdoor thermal comfort studies. As raw data is collected via the mobile measurement tools of map service providers, this approach offers notable advantages such as low cost and high efficiency. However, it also faces limitations due to the delayed updates and limited coverage of Street View images [84].

Overall, compared with traditional methods, the mobile measurement platform, as a type of transportation equipment, not only broadens the application scope of traditional tools for hemispherical photography but also offers advantages such as low cost and

significantly enhances the breadth and efficiency of information acquisition. However, due to varying measurement conditions among different sensors, issues such as insufficient measurement accuracy and inter-device compatibility remain [85]. Non-transient probes typically require sufficient response time to achieve relatively accurate measurements, whereas current mobile measurement platforms, exemplified by drones, usually travel at a constant speed along fixed paths, which may not satisfy the requirements of all sensors during the measurement process.

3.7. Simulation

In studies on OTC, field measurements often impose limitations on the scale and efficiency of the research [86]. Simulation software such as Rayman [20], Skyhelios [87], Envi-met [88], and Grasshopper [4] offer researchers more cost-effective and efficient options for obtaining hemispherical photography [2]. The method of directly constructing hemispherical photography in simulation software using digital elevation models [89], digital ground models [90], and manual 3D modeling techniques [91] presents several advantages: firstly, it reduces costs and minimizes time and labor requirements [92]; secondly, it is not constrained by environmental conditions, enabling large-scale studies to be conducted [93]; lastly, it allows for flexible adjustment of parameters and scenarios while providing immediate validation of study results [94].

However, the simulation software used for constructing hemispherical photography also has limitations. Firstly, during the modeling process, there is a loss of environmental information due to model simplification. In particular, accurately rendering vegetation information in the simulation software proves challenging [32]. Secondly, the accuracy of simulating atmospheric conditions depends on factors such as turbulence and radiation model selection and defining boundary conditions. Often, these simulation conditions need to be adjusted based on field measurement data to enhance their accuracy [2]. Overall, the simulated acquisition of hemispherical photography serves as an effective complement to field measurements by providing a cost-effective means for validating and fine-tuning research outcomes.

3.8. Other Methods

Researchers can utilize software to synthesize multiple ordinary photos into a hemispherical photograph, eliminating the need for specialized equipment and relying solely on everyday photo devices such as smartphones. This approach significantly reduces the cost and complexity associated with constructing hemispherical photographs [95]. The composite photos are primarily created using the open-source panoramic image stitching software “Hugin”, which offers various geometric algorithms (e.g., orthogonal or equidistant projection) to project images onto a flat surface and construct hemispherical photographs [68]. The average similarity between the synthesized hemispherical photography using “Hugin” software and fisheye lens-based acquisition exceeds 91% [54]. Furthermore, Middel et al. employed the panorama image stitching software “PTGui 12 (Panorama Tools Graphical User Interface)” to stitch thermal imager-acquired images into a panoramic image, followed by pixel transformation to synthesize thermal imaging-based hemispherical photography [17]. Li et al. utilized the panoramic image conversion tool “py360convert” to synthesize aerial images acquired by drones into hemispherical photography [4]. Overall, although the method of obtaining hemispherical photography does not necessitate professional fisheye lenses, it still requires post-processing through image-stitching techniques [96].

When capturing luminance information in the environment, researchers can utilize the PhotoLux system to construct hemispherical photography based on luminance. The

optical sensor of the PhotoLux system incorporates a Sigma (Kanagawa, Japan) 4.5 mm F2.8 EX DC CIRCULAR FISHEYE HSM [97]. Boiné et al. employed the PhotoLux system to establish the luminance distribution within an individual's field of view at a pedestrian scale, which still employs a fisheye lens but enhances the comprehensiveness of acquired environmental data [28] (Figure 18).

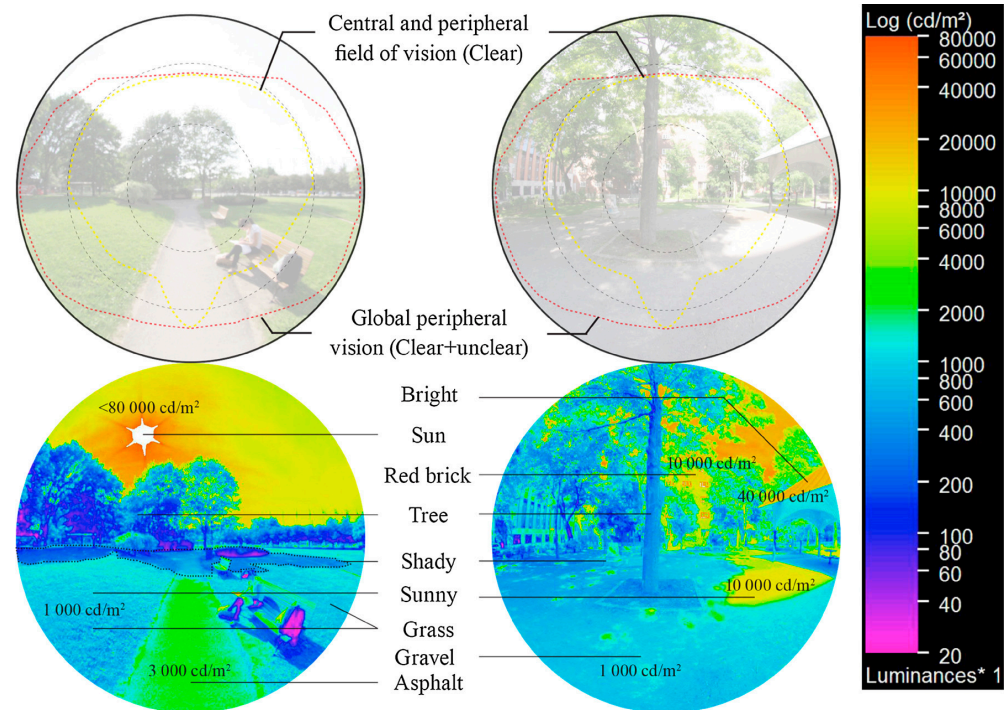


Figure 18. Brightness distribution within the human field of view [28].

In economically disadvantaged areas, researchers can utilize the Spherical Densimeter to obtain hemispherical photography to study canopy density. The device is equipped with either a convex (Model A) or concave (Model C) mirror engraved with 24 one-quarter-inch squares on its surface [98]. Ali et al. demonstrated the low-cost advantage of this method in constructing hemispherical photography for investigating the role of tree canopies in influencing urban microclimate in India (Figure 19) [99].

3.9. Summary

In recent years, the methodologies for constructing hemispherical images in outdoor thermal comfort studies have diversified significantly. These methods encompass fisheye lenses, plant canopy analyzers, Street View images, infrared detection technology, LiDAR, mobile measurement platforms, and simulation software. Each technique possesses distinct advantages that enhance both the accuracy and efficiency of data acquisition. Moreover, these methods cater to a wide range of research scenarios, from microscale to large-scale applications and from high-precision requirements to cost-effective solutions. To achieve an optimal balance between efficiency, accuracy, and cost, it is crucial to select appropriate tools based on specific research contexts (Table 4).



Figure 19. Spherical densiometer with over-head canopy reflection [99,100].

Table 4. Summary of hemispherical photography construction methods.

| Method | Brief Introduction | Advantages | Disadvantages | Applicable Scenarios |
|-----------------------|--|---|--|---|
| Fisheye Lens | Ultra wide-angle lenses, typically with a focal length of ≤ 16 mm, provide an angle of view close to or equal to 180° to obtain hemispherical photography by fixing the camera horizontally or vertically. | As the most traditional method, it has been widely verified in various studies and has the characteristics of high precision. | Limited access, only a small number of fixed points can be covered, high time and labor costs. | Suitable for microscopic research and for recording detailed environmental information at specific points. |
| Plant Canopy Analyzer | Automated acquisition of canopy gap and density information based on optical sensors or fisheye lenses, typical devices such as LAI-2200 and HemiView. | It has a high degree of automation, which effectively reduces human error and is particularly effective in quantitative studies of complex canopy environments. | Expensive equipment, high investment costs, and high dependence on ambient light conditions. | Suitable for complex environments dominated by vegetation. |
| Street View Images | Generation of hemispherical photography by projection methods (e.g., isometric azimuthal projection) using panoramic mapping services such as Google Street View. | It is low cost, has wide spatial and temporal coverage, contains vertical dimensions of information, and is close to real human perception. | Long image update cycle, limited coverage in some areas, only applicable to specific scenes such as vehicular streets. | Applicable to urban microenvironmental studies, taking into account both objective and subjective types of information. |

Table 4. Cont.

| Method | Brief Introduction | Advantages | Disadvantages | Applicable Scenarios |
|-------------------------------|--|---|--|---|
| Infrared Detection Technology | Acquisition of infrared radiation images of objects with thermal imaging cameras. | It is a non-contact measurement with high information density, allowing direct analysis of thermal radiation properties. | Expensive equipment, specific equipment needs to be used in conjunction with a platform (e.g., drones), and the precision of equipment measurements may affect experimental results | Applicable to radiation environment assessment research at the micro-scale. |
| LiDAR | Acquisition of 3D Point Cloud data by laser scanning and processing into hemispherical images using GIS tools. | It is extremely accurate, describes complex urban geometries and vegetation patterns, does not depend on light conditions, and is highly adaptable. | High cost and complicated operation. Data processing is time-consuming and requires specialized technical support. | Suitable for fine-grained urban geometry or vegetation shading analysis. |
| Mobile Measuring Platform | Use drones and unmanned vehicles as vehicles, equipped with a variety of sensors (such as cameras, LiDAR, temperature and humidity sensors) for data collection. | It is flexible and can cover data needs at different heights and locations, improving the efficiency of information acquisition at a lower cost than traditional methods. | The quality of data collection is affected by the stability of the sensors mounted on the platform, and the compatibility of the equipment with the platform needs to be considered. | Suitable for large-scale dynamic environmental data analysis. |
| Simulation | Generation of hemispherical images using modeling tools (e.g., Rayman, Envi-met) or digital terrain models. | It is low-cost and does not require field measurements. It can flexibly adjust parameters to verify and optimize research results. | Simplified models may result in missing critical environmental information. Accuracy is dependent on the model algorithm and initial condition settings. | Suitable for large-scale thermal comfort studies. |
| Others | Compositing hemispherical images using common photo stitching software (e.g., Hugin) or low-cost tools (e.g., spherical densitometer). | It is low-cost, easy to operate, requires no specialized equipment, and can be widely used in scenarios where equipment is scarce or budget is limited. | Lower accuracy, dependent on post-processing quality, with certain requirements on image quality and acquisition conditions. | Suitable for environmental research in areas with low precision or economically backward areas. |

4. Construction of Environmental Information Indicators

4.1. Classification of Environmental Information

Among all the studies, the environmental information constructed using hemispherical photography can be mainly divided into five categories: urban geometry, vegetation, radiation environment, environmental quality, and others. Different environmental information has different impacts on OTC research.

4.1.1. Urban Geometry

Urban geometry plays a pivotal role in regulating the urban heat balance and OTC [101]. In outdoor urban environments, various factors such as building height, density, layout mode, floor-area ratio, H/W ratio, shading measures, and street orientation govern urban geometry [102,103]. Hemispherical photography offers a comprehensive visualization of urban geometry and enables its analysis to establish the relationship between OTC and urban form. Martinelli et al. employed hemispherical photography to construct an accurate representation of urban geometry and concluded that increased building height has a stabilizing effect on OTC [103]. Yan et al., utilizing hemispherical photography, identified building layout mode as one of the primary factors influencing temperature variations within cities [104]. Chatzidimitriou et al., through hemispherical photography analysis of Greek streets, determined that streets oriented along the NW-SE axis were favorable for summer thermal comfort [105]. Overall, hemispherical photography provides a precise

and effective means to depict urban geometry in studies related to thermal comfort [106], serving as a foundation for further analyses.

4.1.2. Vegetation

The vegetation in urban outdoor environments typically comprises street greening (street trees, shrubs, grass), parks, gardens, forests, and rooftop greening [107,108]. Vegetation plays a crucial role in terms of urban OTC [109], with its impact being influenced by factors such as tree height, canopy width, plant shading, transpiration rate, and leaf area index [110]. It has been pointed out that vegetation area is a key factor in urban cooling [111], parks with more regular shapes have better cooling effects [112], and tree canopy area is more effective in cooling than the number of leaf layers [113].

Hemispherical photography provides a realistic means to gather information on tree height, leaf density, tree shading effects, canopy overlap patterns, etc., which can be utilized for conducting detailed analysis of vegetation and OTC. Liu et al. employed hemispherical photography to analyze tree planting methods and concluded that the layout should maximize shaded areas while avoiding unnecessary canopy overlap and considering the planting direction to enhance the cooling capacity of trees [114]. Yang et al.'s study in China using hemispherical photography revealed that the cooling effect of vegetation gradually diminishes when the ratio of tree height to building height exceeds approximately 1:2 [115]. Comparing building shade with vegetation shade through hemispherical photography techniques in Hong Kong demonstrated that vegetation shade has a greater potential for reducing UTCI (Universal Thermal Climate Index) levels [116]. Stocco et al. used hemispheric photography to screen solar radiation environments in their study in Argentina and found that people in urban plazas with a high percentage of green space felt more comfortable and had a 16% higher percentage of people who felt comfortable under the same conditions of solar radiation [102].

4.1.3. Radiation Environment

The urban outdoor radiation environment is a crucial component of the urban microclimate and physical environment, exerting a significant impact on the urban energy balance and human thermal comfort [117]. This complex radiation environment is typically influenced by various factors, including direct solar radiation, diffuse radiation, solar trajectory, atmospheric conditions [118], longwave radiation from urban structures, and the ground cover in the urban subsurface layer [119]. OTC exhibits substantial variations due to different seasons, emission sources, and radiation directions [120]. Hemispherical photography enables the acquisition of ground-level radiation information at varying surface albedos [121], facilitating analysis of the influence of radiative environments on OTC. Kim et al. discovered that in low sky view factor (SVF) urban canyons, heat loads experienced by pedestrians were primarily attributed to radiative emissions from walls and floors [122]. Vieira et al., through hemispherical images captured with a fisheye lens, compared cooling capacities among different plant species and found that disparities mainly originated from distinct shading abilities against solar radiation [123].

4.1.4. Environmental Quality

Environmental quality is an objective assessment of the environment based on individuals' subjective perception of outdoor spaces, which is influenced by various factors such as landscape characteristics, built structures, streetscape elements, sky conditions, and solar exposure [124]. It serves as a metric for human evaluation of environmental quality that impacts both psychological and physiological aspects of outdoor pedestrian thermal comfort [104,125]. Hemispherical photography offers a convenient approach to quantifying environmental quality as it provides a visual field similar to human eye observation [28].

Kim et al. conducted a statistical analysis using the hemispherical photography method to assess large-scale spatial environmental quality in Tokyo, Japan, and found that the cooling effect of greenery improves when it exhibits a more clustered, fragmented, and complex spatial pattern, indicating a higher environmental quality [124]. Niu et al., after utilizing hemispherical photography to capture environmental information in Chongqing, China, discovered that aesthetically pleasing landscapes and well-designed features contribute to enhanced satisfaction with green spaces. Moreover, high environmental quality not only mitigates thermal discomfort during summer but also increases people's frequency of physical activity [126].

4.1.5. Others

Hemispherical photography also enables the characterization of individuals [48], temporal variations [28], meteorological conditions [127], seasonal changes [128], and societal disparities [129] in images, which are environmental factors that have minimal impact on OTC or are beyond human control.

There are significant variations in the factors influencing outdoor thermal comfort under different climatic conditions. Studies have shown that hemispherical photography can effectively capture environmental information, but its impact on climatic conditions varies. For instance, Chen et al. found that under high-altitude cold climatic conditions, using hemispherical photography to characterize ground surfaces resulted in a less pronounced improvement in the thermal environment, with even lawns failing to produce a notable cooling effect [130]. Environmental factors affecting outdoor thermal comfort can differ markedly between seasons within the same region. Liu et al. employed hemispherical photography for long-term street observations and discovered that the influence of street canyon width on solar radiation intensity varies with seasons, being more pronounced during transitional and cold seasons (September to May) compared to the hot season (June to August), with a stronger effect observed during colder periods [131].

Hemispheric photography construction methods based on field measurements are influenced by weather conditions when describing environmental information. The intervening effect of different weather conditions not only impacts outdoor thermal comfort [132] but also affects the accuracy of measurement instruments [133]. Drach et al. in the UK collected outdoor environmental data through hemispherical photography under various weather conditions and found that windy and cloudy conditions diminished the influence of ground cover on temperature patterns [42]. Tan et al. in China utilized hemispherical photography to gather vegetation information for both sunny and cloudy days, revealing that the cooling capacity of trees with high and low sky view factors (SVFs) varied under different weather conditions [134]. Lam et al. in Australia employed hemispherical photography to assess human visual comfort and discovered that while solar radiation significantly influences human heat balance, visual comfort also plays a crucial role in outdoor thermal comfort [135].

Overall, the influence of environmental factors such as climate and weather conditions on outdoor thermal comfort should not be underestimated. These factors play a crucial role in determining outdoor thermal comfort in specific situations [136].

4.2. Selection of Environmental Information Indicators

In studies on OTC, environmental information indicators aim to provide a comprehensive depiction of human perceptions and sentiments towards the urban outdoor environment; however, hemispheric photography alone cannot fully capture all aspects of the environment [137]. Amongst the papers included in this study, hemispherical photography was primarily utilized to describe urban geometry, vegetation, radiation environment,

seasonal climate, and environmental quality. Notably, it was most frequently employed for depicting urban geometry and vegetation information (Figure 20).

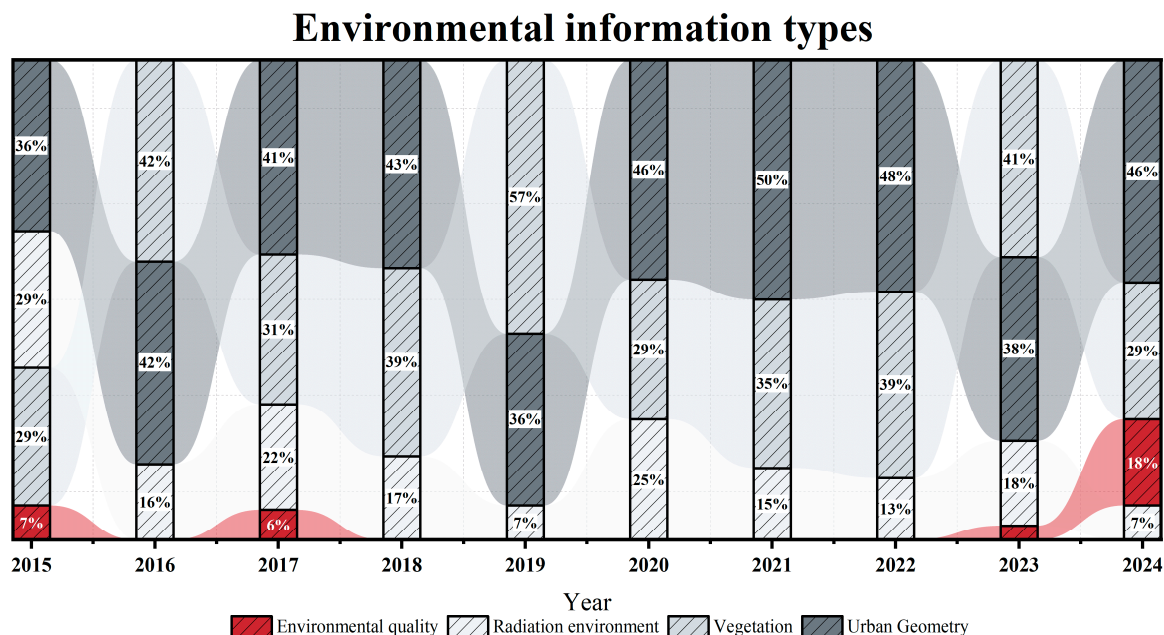


Figure 20. Trends in changes in environmental information.

As depicted in Figure 21, SVF emerges as the predominant and extensively employed comprehensive index for environmental information across all studies. Moreover, SVF is widely acknowledged as a key physical parameter influencing thermal comfort in urban streets [138], with even studies utilizing alternative indicators still incorporating SVF measurements for comparative analysis [37]. However, despite its comprehensiveness in characterizing urban form, certain studies have highlighted that SVF alone fails to provide an accurate depiction of the urban environment [51]. For instance, Song et al. demonstrated that due to the absence of crucial environmental factors such as airflow, building characteristics, and vehicular heat emissions within SVF calculations, it is imperative not to overlook this informational deficiency when describing the urban environment [139]. Furthermore, Yan et al. emphasized that relying solely on SVF values cannot precisely quantify urban environmental information; instead, a combination of sky view factor (SVF), building view factor (BVF), and tree view factor (TVF) should be incorporated to enhance accuracy [104].

In addition to utilizing SVF for synthesizing diverse environmental information, hemispherical photography can provide numerous specialized indices for characterizing various aspects of the environment. For instance, vegetation in the environment can be described using indices such as LAI [35], TVF [10], GPR [140], LAD [141], canopy density [99], VVF [39], and PAI [123]. Radiation in the environment can be described using TSF [140], PAR [142], and SunPath [105]. Environmental quality can be assessed through indices like SVI [143] and GVI [143]. Overall, hemispherical photography enables the construction of multiple environmental information indices to achieve a comprehensive depiction of urban environments (Table 5) [144].

Environmental information indicators

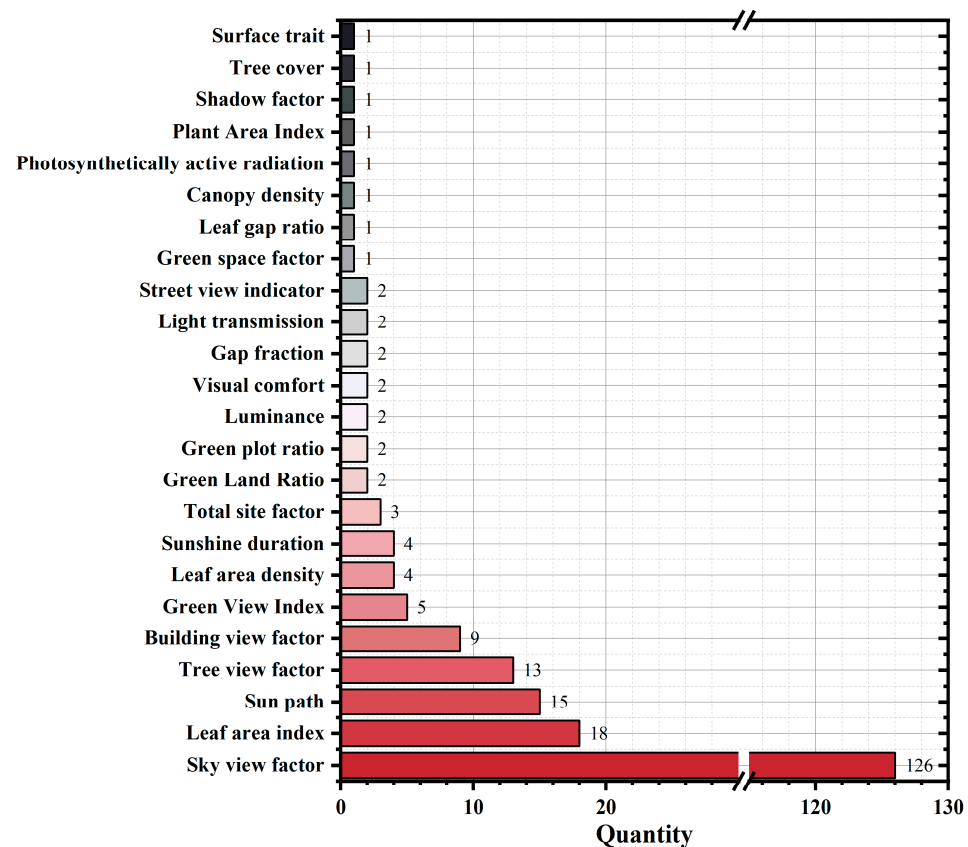


Figure 21. Frequency of research on environmental information indices.

Table 5. Environmental information indices obtained using hemispherical photography.

| Abbreviation | Environmental Information Indices | Brief Introduction | Number of Studies | Environmental Information |
|--------------|-----------------------------------|---|-------------------|--|
| SVF | Sky view factor | SVF is a dimensionless parameter that represents the proportion of the overlying hemisphere occupied by an open sky at any point in a given location. Some other derived metrics are included (Such as Horizontal SVF and Park SVF). | 126 | urban geometry, vegetation, radiation, environmental quality |
| LAI | Leaf area index | LAI is a dimensionless metric to quantify leaf density and complexity in the vegetation canopy. | 18 | vegetation, radiation |
| SP | Sun path | The path of the sky through which the sun rises from the horizon until it sets again. | 15 | radiation |
| TVF | Tree view factor | TVF is used to characterize the shading coefficient of a tree canopy. It references the concept of SVF, which is the proportion of the overlying hemisphere occupied by the vegetative canopy. Some other derived metrics are included (Such as the SVF and Vegetation view factor). | 13 | vegetation, |
| BVF | Building view factor | The BVF is used to characterize the visual accessibility of a building's surfaces, and it references the concept of SVF, which is the proportion of the overlying hemisphere that is occupied by the building's surfaces. Some other derived metrics are included (Such as SVF building and artificial material view factor). | 9 | urban geometry |
| GVI | Green View Index | GVI is used to quantify the distribution and density of green vegetation in a given area. | 5 | vegetation, environmental quality |
| LAD | Leaf area density | LAD is used to characterize the total leaf area of vegetation per unit volume and provides more detailed three-dimensional spatial information compared to LAI. | 4 | vegetation, radiation |

Table 5. Cont.

| Abbreviation | Environmental Information Indices | Brief Introduction | Number of Studies | Environmental Information |
|--------------|-------------------------------------|---|-------------------|--|
| SD | Sunshine duration | SD is the length of time that direct solar radiation reaches the ground in a given period. | 4 | radiation |
| TSF | Total site factor | TSF refers to the ratio of radiation received under the canopy to that received above the canopy on an average daily basis and is used to quantify the incident radiation that penetrates the obstruction and is a composite parameter that integrates spatial geometry, vegetation, solar trajectory, and the intensity and timing of solar radiation. | 3 | urban geometry, vegetation, radiation |
| GLR | Green Land Ratio | GLR refers to the amount of green plants perceived by the human eye and is an index of landscape characteristics that measures the vegetation content of the spatial environment. | 2 | vegetation, |
| GPR | Green plot ratio | GPR is used to assess the percentage of green space (e.g., vegetation and parks) in a city or development relative to the total floor area or parcel size. | 2 | vegetation, |
| / | Luminance | Refers to the light intensity perceived by the human eye, describing the brightness of a surface or light source in a specific direction. | 2 | radiation, environmental quality |
| VC | Visual Comfort | It is a subjective feeling that refers to the comfortable, non-fatiguing, non-irritating visual sensation felt by the human eye under specific light conditions. | 2 | environmental quality |
| GF | Gap fraction | Refers to the proportion of the area of unobstructed sky or ground that can be seen through vegetation canopy or other obstructions in the overlying hemispheric image. | 2 | vegetation, radiation |
| LT | Light transmission | Refers to the amount of light that penetrates the tree canopy. | 2 | vegetation, radiation |
| SVI | street view indicator | A composite metric that combines multiple metrics to describe streetscape information. | 2 | urban geometry, vegetation, radiation, environmental quality |
| GSF | Green space factor | An index used to assess the quantity and quality of green space in an urban or built environment is usually described in terms of the proportion of green space visible in the field of view. | 1 | vegetation, environmental quality |
| LGR | Leaf gap ratio | LGR is commonly used to describe the ratio of gaps between leaves in a plant leaf arrangement. | 1 | vegetation, radiation |
| CD | Canopy density | The CD is an index that describes the degree to which the tree canopy covers the ground in a forest. | 1 | vegetation, radiation |
| PAR | photosynthetically active radiation | PAR is the energy of light in the spectral range of wavelengths between 400 and 700 nanometers. | 1 | vegetation |
| PAI | Plant Area Index | It is an index used to describe the ratio of the total area of leaves or other photosynthetic organs in a plant population to the surface area, similar to the leaf area index (LAI), but PAI can be more widely applied to include other plant parts besides leaves. | 1 | vegetation, radiation |
| SF | shadow factor | A measure that describes the degree of shading of a surface, that is, the proportion of direct solar radiation received by the surface reduced due to the presence of surrounding obstacles. | 1 | radiation |
| TC | tree cover | The total area of tree branches and foliage projected on the ground as a proportion of the total area of the study area is usually expressed as a percentage. | 1 | vegetation |
| ST | surface trait | Refers to characteristics such as surface material, color, and scale. | 1 | environmental quality |

4.3. Construction of Environmental Information Indices

Hemispherical photography, as an objective recording of image data of the environment, usually requires the processing of images with the help of different software tools or artificial intelligence algorithms, which are used to realize the construction of environmental information indicators.

4.3.1. Construction of Environmental Information Indices Based on Traditional Software

As depicted in Figure 22, among all the studies, the Rayman software developed by Matzarakis et al. in 2000 remains the most extensively employed comprehensive tool for hemispherical photography processing. In terms of describing vegetation-related environmental information, WinSCANOPY and plant canopy analysis are relatively more prevalent. In recent years, with the rapid advancement of OTC studies employing Street View images, algorithmic programming tools such as machine learning have gradually gained acceptance among researchers.

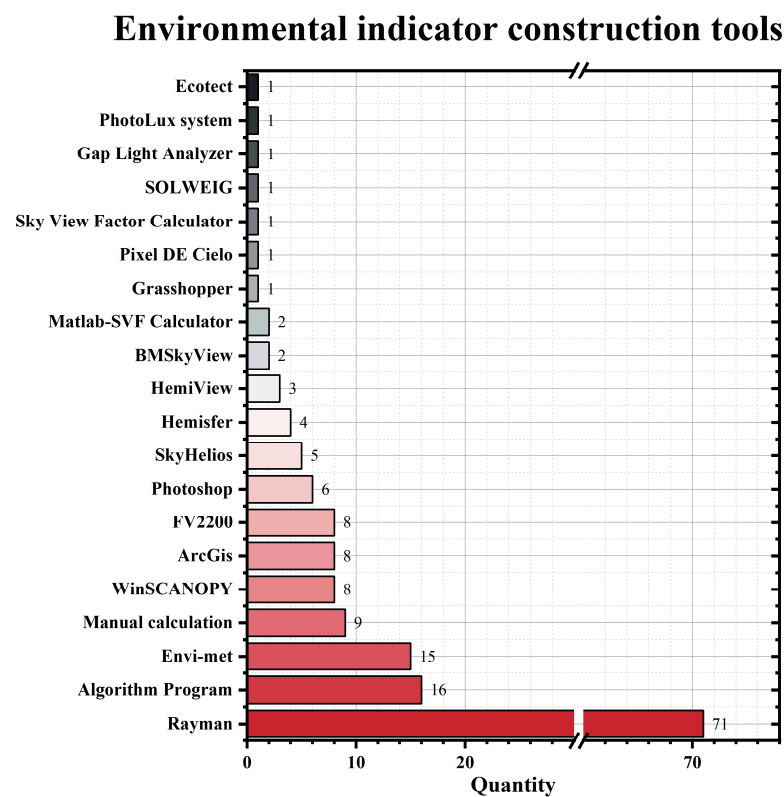


Figure 22. Frequency of use of tools for constructing environmental information indices.

In general, when constructing environmental information indices using hemispherical photography in OTC studies, it is crucial to consider not only the quantification ability of different tools for visual information of the environment but also the study's purpose and specific environmental characteristics. Selecting appropriate software is essential to enhance the accuracy of environmental descriptions. While generalized and comprehensive indices and their construction tools are commonly employed, researchers in specific environmental fields and with distinct research objectives also appreciate specialized indices and tools that offer higher accuracy.

4.3.2. Construction of Environmental Information Indices Based on Artificial Intelligence

In the past decade, artificial intelligence (AI) and algorithmic programs have been increasingly utilized in hemispherical photography-based outdoor thermal comfort re-

search to construct environmental information indices. Specifically, algorithms such as “DeepLab” [32], “PSPNet” [131], “SegNet” [124], “SegFormer” [143], and other widely used semantic segmentation models from the field of computer vision have been employed to classify and annotate hemispherical photographic images, thereby enabling the automated construction of relevant environmental information indicators. Despite AI’s current limited adoption (11%), its demonstrated high efficiency and accuracy in processing large or continuous datasets make it a promising direction for future research.

In 2017, Liang et al. introduced a method for automatically extracting sky view factors (SVFs) from Google Street View images using the SegNet deep learning model [86]. Since then, AI has increasingly been applied to passive mobility measurement research, particularly in studies utilizing Street View imagery. Gong et al. developed a PSPNet-based approach for classifying and recognizing image information from Google Street View, subsequently generating hemispherical images and extracting SVF, TVF, and BVF [145]. Zeng et al. created a sky region detection tool using Python and OpenCV [146], while Xia et al. employed DeepLabV3+ for classifying and analyzing Street View images [147]. The majority of studies leveraging Street View images have utilized AI techniques to enhance both efficiency and accuracy. Given AI’s superior performance in big data processing, it has demonstrated strong adaptability in active mobile measurement studies conducted on mobile platforms. Song et al. proposed an environmental information acquisition method based on deep learning for hemispherical photography [39]. Li et al. developed a drone-based measurement method combined with algorithmic procedures for constructing environmental information [4]. Zhong et al. introduced a machine learning model to improve the accuracy of acquiring urban microscale environmental data via drones [148]. Additionally, Witzmann et al. developed an algorithm to optimize LiDAR modeling for sub-canopy solar radiation analysis [149].

Overall, the current application of artificial intelligence in outdoor thermal comfort research utilizing hemispherical photography primarily achieves efficient and high-precision processing of large volumes or continuous image data by incorporating semantic segmentation models. This approach automates relevant processes, thereby significantly enhancing the accuracy and efficiency of constructing pertinent environmental information.

5. Discussion

5.1. Transformation in Hemispheric Photography Construction Methodology

Among the 142 papers included in this study on hemispherical photography construction methods, 107 opted for acquiring hemispherical photography through a fisheye lens. Using a fisheye lens remains the predominant approach for constructing hemispherical photography; however, more studies now employ other tools to capture more comprehensive information (Figure 23). These novel approaches often enable simultaneous acquisition of multiple environmental parameters or facilitate easier data retrieval. Plant canopy analyzers offer efficient means for vegetation characterization and automated data processing under various weather conditions [57]. Infrared detection techniques can differentiate between longwave and shortwave radiation, providing accurate characterization of radiative environmental information [17]. LiDAR techniques allow for modeling complex structures such as trees [18], while the PhotoLux system enables precise acquisition and visualization of environmental brightness information [28]. Additionally, the Blue IR filter is employed with the fisheye lens to replace the camera’s hot mirror and capture dual-wavelength images, thereby obtaining more extensive environmental information [31].

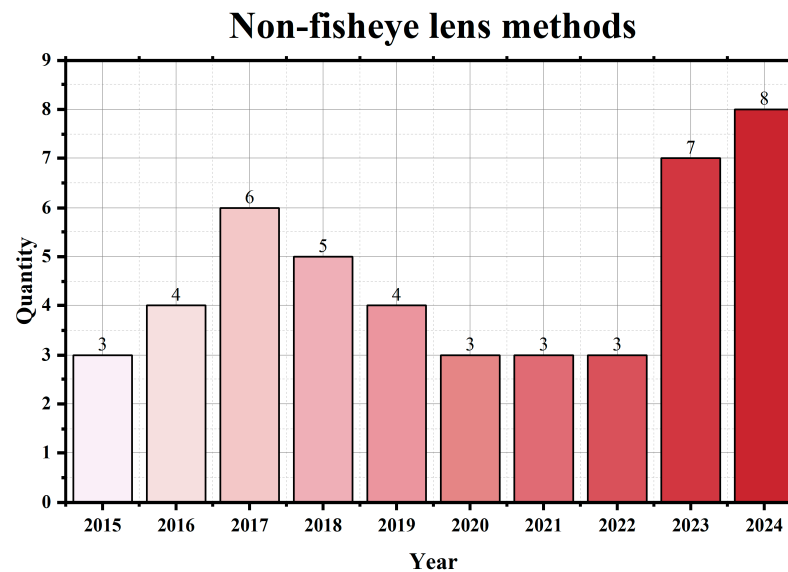


Figure 23. Trends in non-fisheye lens methods.

The utilization of simulation software for acquiring hemispherical photography, as a widely adopted conventional approach not constrained by physical environmental conditions, offers the advantages of cost-effectiveness and high efficiency. However, the process of constructing a simplified model encounters limitations such as inadequate accuracy in simulating atmospheric conditions and incomplete model information [92]. In recent years, only 13% of the studies have exclusively utilized hemispherical photography simulation software, with the majority employing it as a cost-effective approach to validate spatial optimization strategies.

Due to constraints in time and labor costs, the application of fisheye lens-based hemispherical photographic construction methods is typically limited to a few fixed points, resulting in short periods and small spatial scales [150]. In the past, this issue was addressed by employing simulation software to simulate large-scale spaces over extended periods. However, the simplified model used during the modeling process lacked information, leading to inaccuracies and deficiencies [2,32]. To acquire more precise information regarding large-scale urban environments, there has been a significant increase in papers focusing on mobile measurements for extensive field studies on OTC (Figure 24).

Mobile measurements can be broadly classified into active and passive approaches. Active mobile surveying involves the researcher personally acquiring continuous hemispherical photography or video using mobile surveying platform tools such as drones, bicycles, carts, etc., which enable rapid movement in urban spaces. This method can be complemented by emerging technologies like infrared detection and LiDAR technology. Equipping corresponding sensors on the mobile surveying platforms facilitates the acquisition of more comprehensive environmental information.

On the other hand, passive mobile measurement typically relies on Street View images obtained directly by researchers to gather large-scale urban environmental data. While this approach is cost-effective and highly efficient since it utilizes original information acquired from map service providers through mobile measurement, it is limited by delayed updates of Street View images themselves and restricted coverage areas. Consequently, these limitations somewhat impede the timeliness of constructing hemispherical photography through passive mobile measurement as well as its applicability [84].

Mobile measurement methods

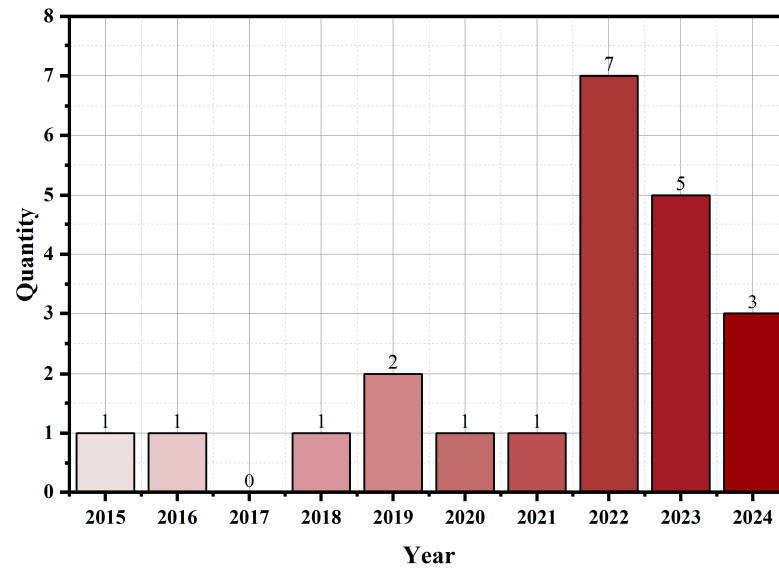


Figure 24. Trends in mobile measurement methods.

5.2. Transformation of the Process of Constructing Environmental Information Indices Based on Hemispherical Photography

The role and significance of hemispherical photography in the construction of environmental information indices is transforming in all studies. Presently, 18% of all papers employ hemispherical photography solely as a comparative tool to validate the accuracy of modeled environments, no longer actively participating in the process of constructing subsequent environmental information indices. Furthermore, there is a declining trend in the proportion of studies that provide comprehensive descriptions or visual representations (such as images) of hemispherical photography and its acquisition methods, with an increasing number opting to utilize hemispherical photography exclusively to construct environmental information indices without providing detailed explanations (Figure 25).

Description of frequency of hemispherical photography

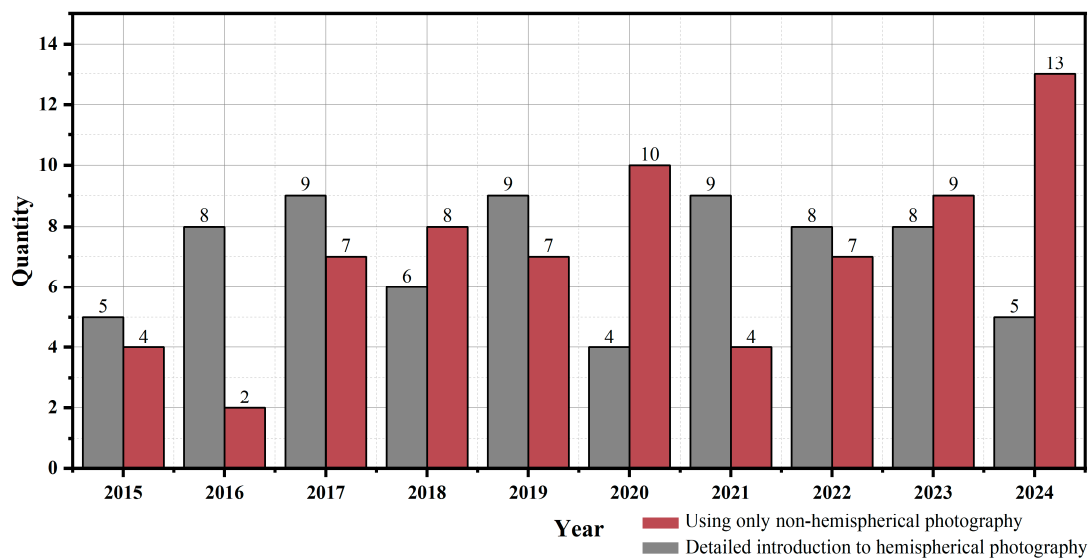


Figure 25. Detailed/non-detailed description of frequency of hemispherical photography.

In constructing indices for environmental information, 88% of studies develop at least one comprehensive index represented by the SVF. The SVF was initially devised by Steyn

in 1980 based on fisheye lens images [151], and a simplified computational approach was subsequently introduced by Chapman et al. in 2001, which is currently the most widely adopted method [152]. While SVF offers advantages such as broad applicability and quick computation, it has gradually revealed its limitations in describing urban environmental information as research on OTC deepens [51]. Furthermore, the traditional generalized index represented by SVF fails to adequately consider subjective environmental information captured through hemispheric photography. Nikolopoulou and Steemers discovered that only 50% of variations in outdoor pedestrian thermal sensation could be explained by objective environmental parameters in studies on OTC, highlighting how outdoor environmental quality influences individuals' perception of thermal comfort [153]. A Brazilian study demonstrated significant statistical differences in respondents' thermal sensation ratings at locations with similar SVFs but varying morphological characteristics [27]. Manavvi et al.'s research conducted in India further revealed that human subjective perceptions of visual elements such as architectural proportions, materials, colors, lighting, and landscaping components significantly influence OTC. However, some studies have also indicated that solely considering subjective environmental factors does not accurately capture changes in OTC [154]. Overall, while objective physical factors predominantly govern OTC, the impact of subjective psychological factors on this aspect cannot be disregarded; thus, effective development of environmental information indices necessitates a comprehensive depiction of both objective and subjective environmental information [138].

In all the studies, while almost all of them employed hemispherical photography to construct objective environmental information indices, there has also been a significant increase in the number of studies that have utilized subjective environmental information indices based on pedestrian perspectives in recent years (Figure 26). Hemispherical photography serves as a tool for subjectively expressing the real environment from a pedestrian's viewpoint. Its field measurements and image properties closely approximate those of human vision and enable effective quantification of subjective human perception regarding visual and psychological factors [155]. This previously challenging task of quantifying the interaction between visual and thermal sensations holds important implications for researchers and urban planners [135].

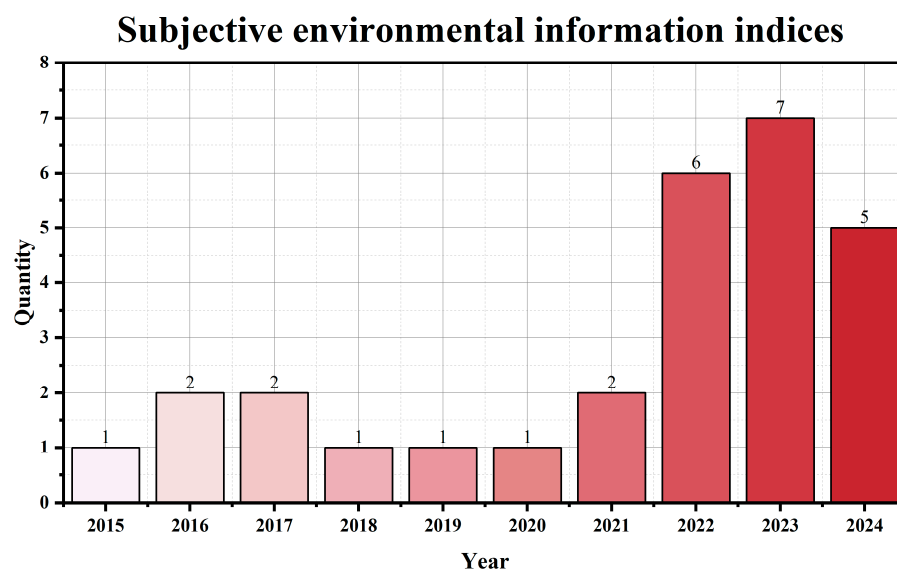


Figure 26. The trend of subjective environmental information indices.

Overall, with the deepening of OTC research, human thermal exposure has begun to show significant spatial variability, and it will be increasingly important to quantify human

subjective thermal sensations at the micro-scale level [37]. Hemispherical photography, as a means of describing environmental information, has good accuracy in constructing objective environmental information indices [31], and at the same time, it has the characteristics of a viewing angle that is similar to, and slightly larger than, that of the human eye when measured in the field [28], which gives it significant advantages in quantifying the visual information of the environment as perceived by human beings and in constructing subjective environmental information indices.

5.3. Transformation of the Process of Constructing OTC Indices Based on Hemispherical Photography

In the field of OTC research, there exist diverse definitions of thermal comfort for the human body. Fanger (1970) defined thermal comfort as a state where all heat inflows (gains) and outflows (losses) from the body are in equilibrium, taking into account environmental factors and physiological regulation of body temperature within a specific range [6]. Conversely, ASHRAE (2009) defined thermal comfort as “the psychological state of being satisfied with one’s thermal surroundings”, which considers physical, personal, social, and psychological factors [12]. Existing indices for assessing thermal comfort are commonly classified as objective (based on steady-state heat transfer models, dynamic-based heat transfer models, and regression models derived from hot and cold environments) or subjective [156].

In recent years, studies on urban OTC have revealed that while microclimatic parameters primarily influence human OTC through physical environmental factors, non-physical environmental factors encompassing social, psychological, and personal aspects also play a significant role [157]. Regarding physical environmental factors, it is essential to consider human and biometeorological conditions holistically by balancing heat production and dissipation. This includes considering variables such as human metabolic rate, thermo-physical properties of clothing, air temperature, average radiant temperature, wind speed, and relative humidity [10]. Non-physical environmental factors typically involve social (e.g., academic background and economic level), psychological (e.g., thermal history), and personal (e.g., age and gender) aspects. Additionally considered are individual factors like clothing choices and activities, social elements such as companionship and mode of transportation, psychological aspects including time of exposure (ToE), frequency of visit (FoV), overall satisfaction levels with the environment’s thermal conditions, and purpose of visit (PoV) [11].

The utilization of thermal comfort indices in the papers included in the study is depicted in Figure 27. Objective evaluation indices prevail, being employed approximately 3.2 times more frequently than subjective evaluation indices. However, notwithstanding the overall, albeit limited, frequency of employment of subjective evaluation indices, there has been a rapid surge in their acceptance in recent studies from 2022.

Ninety-eight percent of all published studies included at least one objective thermal comfort evaluation index. Among these, PET, a generalized index primarily used for indoor environments, and traditional microclimate indices such as air temperature, wind speed, and radiant flux (Figure 28) were the most commonly employed. However, there has been a rapid increase in the utilization of specialized indexes like UTCI that have been specifically developed for outdoor environments (Figure 28). TSV remains the frequently used subjective evaluation index; however, recent years have witnessed the emergence of subjective indices such as attendance, PANAS (Positive and Negative Affect Schedule), MVPA (moderate to vigorous physical activity), etc., which indirectly capture human perception of OTC.

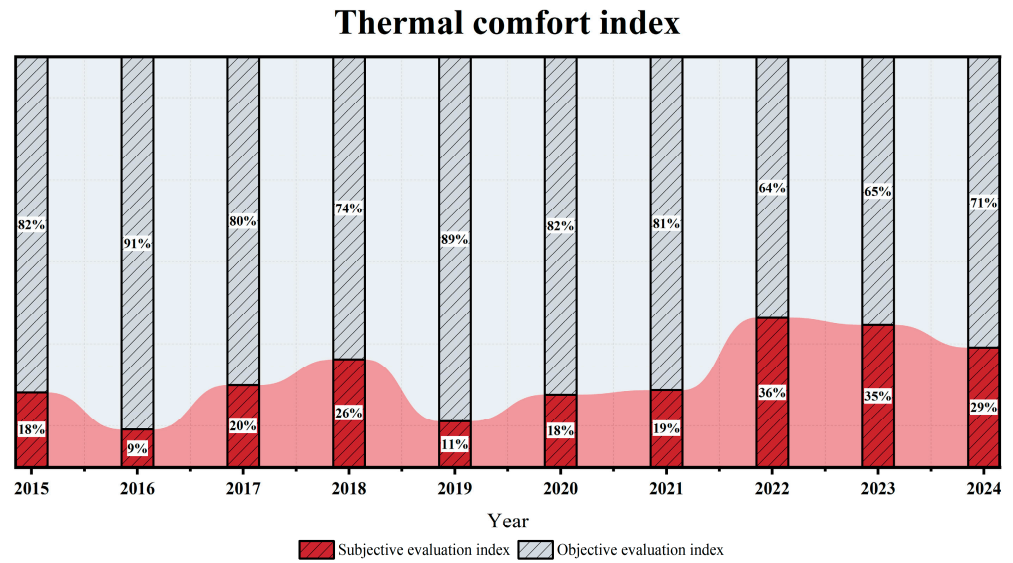


Figure 27. Trends in thermal comfort index.

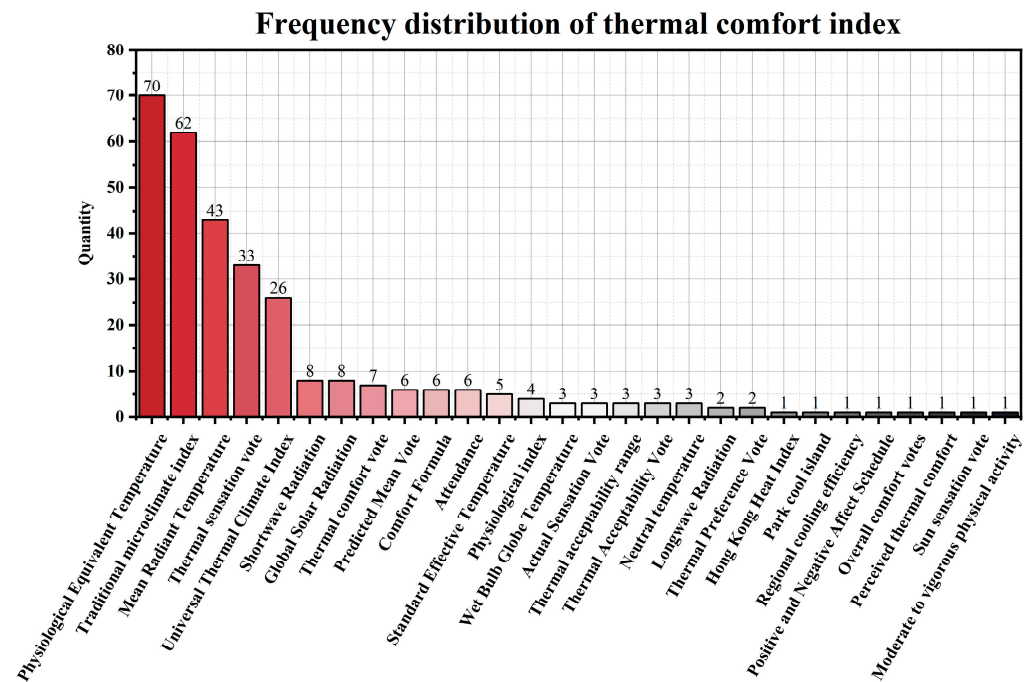


Figure 28. Frequency distribution of thermal comfort index. Note: Traditional microclimate index includes air temperature, relative humidity, wind speed, dry-bulb temperature, wet-bulb temperature, surface temperature, ground surface temperature, UVA/UVB, and vapor pressure. Deficit and other traditional microclimate indices.

Despite the predominant influence of physical environmental factors on OTC, there is currently no universally recognized index for evaluating this aspect [158]. While existing thermal comfort indices based on physical parameters and steady-state models have been extensively studied, they have proven inadequate in accurately describing OTC. Conversely, dynamic and non-stationary models that closely align with human thermophysiological parameters exhibit relatively higher accuracy in OTC research [159]. Nevertheless, the steady-state model remains the primary thermal index employed in practical studies on OTC. For instance, PET (Physiological Equivalent Temperature), as a comprehensive index that is computationally straightforward and encompasses a wide range of perceived temperature sensations or pressure categories [7], has been utilized as an index for assessing

OTC in over 49% of all studies. However, several studies have demonstrated that PET's reliance on a steady-state-based model limits its ability to accurately evaluate dynamically changing variations in OTC [59].

In the current stage of OTC studies, researchers primarily prioritize the practicality and versatility of thermal comfort indices over their accuracy. However, combining subjective and objective thermal comfort indices can usually achieve a comprehensive reflection of OTC conditions [46].

5.4. Transformation of Urban Space Optimization Strategy Based on Hemispherical Photography

Studies with urban space optimization strategies as their research objectives (41% of the articles) usually grouped optimization strategies into five categories: urban geometry, vegetation, radiation environment, environmental quality, and other related elements. Hemispherical photography, as a method that integrates objective and subjective environmental information, derives urban space optimization strategies that pay close attention to the cross-modal balance of human sensory temperature, visual comfort, and thermal comfort. The data-driven nature of the optimization strategy also motivates urban planners and urban designers to use hemispherical photography and microclimate models to accurately measure the impact of vegetation and urban geometry on thermal comfort, optimize the design parameters, and develop site-specific solutions. Some studies have further combined artificial intelligence and big data technologies to enable dynamic environmental monitoring and prediction to improve the adaptability and effectiveness of optimization strategies.

The urban space optimization strategy derived from hemispherical photography will regulate all kinds of environmental factors through multi-scale design strategies to build a human-centered urban space optimization system. In the future, it will continue to develop, focusing on refined design, data-driven and intelligent design, and urban sustainability and eco-efficiency.

This study acknowledges several limitations. Firstly, it only reviewed outdoor thermal comfort studies utilizing hemispheric photography methods from the past decade, potentially overlooking foundational research or significant findings published earlier. Secondly, the selected literature predominantly focuses on specific urban environments, with limited coverage of rural and peri-urban areas, which may restrict the global applicability of the findings. Future research should aim to broaden the scope of subjects to enhance the wider application of hemispherical photography in environmental monitoring and urban design.

6. Conclusions

This study provided a comprehensive synthesis of the research conducted in the past decade on the utilization of hemispherical photography for urban OTC studies. Furthermore, it elucidates the evolution of hemispherical photography in this field by comparing and contrasting various tools and methodologies.

1. Researchers are increasingly concerned about the versatility of hemispherical photography construction methods rather than solely focusing on their accuracy. In economically disadvantaged regions, researchers need to pay additional attention to the cost-effectiveness of hemispherical photography construction. Although the fish-eye lens remains crucial for constructing hemispherical photography, its combination with other measurement tools is transforming it from a purely visual image into a composite image that provides richer information. The utilization of simulation software to construct hemispherical photographs is evolving as an affordable approach to validate spatial optimization strategies;

2. Motion measurement has been incorporated into the construction methodology of hemispherical photography, enabling a shift from fixed-point research based on limited data points to large-scale investigations encompassing entire regions through the utilization of active mobile measurement tools such as drones equipped with fisheye lenses and bicycles, as well as passive mobile measurement tools like Street View images;
3. Among the environmental information indices derived from hemispheric photography, the prevailing generalized and comprehensive indices are still represented by SVF. However, researchers have recognized the limitations of SVF in providing a comprehensive description of environmental information, leading to the adoption of a more targeted index;
4. Although most studies have constructed objective environmental information indices, the use of subjective environmental information indices based on pedestrian perspectives is also increasing rapidly. Hemispherical photography is based on the image of the approximate field of view range of the human eye obtained from real measurements, which enables it to show its effectiveness and convenience in describing subjective environmental information beyond other methods;
5. In OTC studies based on hemispherical photography, researchers emphasize the practicality and versatility of thermal comfort indices rather than their accuracy. Although objective thermal comfort indices still dominate, the combination of subjective thermal comfort indices can provide a more comprehensive response to the OTC status, and hemispherical photography has advantages in constructing subjective thermal comfort indices.

Overall, hemispherical photography remains a critical traditional outdoor thermal comfort research method. However, future research should focus on enhancing the generalizability of this method rather than solely emphasizing information acquisition precision, particularly in economically disadvantaged regions where hemispherical photography can be conducted conveniently, efficiently, and cost-effectively. Additionally, researchers should leverage diverse mobile measurement techniques to extend both the temporal and spatial scope of studies, transitioning from small-scale point-based analyses to broader regional assessments to enhance study reliability and accuracy. Finally, when constructing environmental information indicators and screening thermal comfort indicators, greater emphasis should be placed on the unique advantages of hemispherical photography, which captures an approximate field of view similar to that of the human eye. This approach can deepen and broaden the study by developing subjective environmental and thermal comfort indicators, ultimately providing more human-centered design strategies for optimizing urban spaces.

Author Contributions: Conceptualization, Y.L., L.S. and X.S.; data curation, Y.L. and X.S.; chart drawing, X.S. and Y.L.; funding acquisition, L.S.; literature screening, X.S.; project administration, L.S.; resources, Q.Y. and Y.L.; software, X.S. and Y.Z.; supervision, L.S.; writing—original draft, Y.L. All authors have read and agreed to the published version of the manuscript.

Funding: This research was financially supported by the National Natural Science Foundation of China (Grant No. 52078344).

Data Availability Statement: The data presented in this study are available on request from the corresponding author. The data are not publicly available due to privacy.

Conflicts of Interest: The authors declare no conflicts of interest.

Abbreviation

| | |
|-------|-------------------------------|
| OTC | outdoor thermal comfort |
| LAI | leaf area index |
| GIS | geographic information system |
| LiDAR | light detection and ranging |
| SVF | sky view factor |
| TLS | terrestrial laser scanning |

References

- Baklanov, A.; Molina, L.T.; Gauss, M. Megacities, Air Quality and Climate. *Atmos. Environ.* **2016**, *126*, 235–249. [CrossRef]
- Vurro, G.; Carlucci, S. Contrasting the Features and Functionalities of Urban Microclimate Simulation Tools. *Energy Build.* **2024**, *311*, 114042. [CrossRef]
- Giannaros, C.; Nenes, A.; Giannaros, T.M.; Kourtidis, K.; Melas, D. A Comprehensive Approach for the Simulation of the Urban Heat Island Effect with the WRF/SLUCM Modeling System: The Case of Athens (Greece). *Atmos. Res.* **2018**, *201*, 86–101. [CrossRef]
- Li, K.; Liu, M. Combined Influence of Multi-Sensory Comfort in Winter Open Spaces and Its Association with Environmental Factors: Wuhan as a Case Study. *Build. Environ.* **2024**, *248*, 111037. [CrossRef]
- de Dear, R.; Brager, G.S. Developing an Adaptive Model of Thermal Comfort and Preference. 1998. Available online: https://www.researchgate.net/publication/269097185_Developing_an_Adaptive_Model_of_Thermal_Comfort_and_Preference_-_Final_Report_on_RP-884 (accessed on 10 July 2024).
- Fanger, P.O. *Thermal Comfort: Analysis and Applications in Environmental Engineering*; Danish Technical Press: Copenhagen, Denmark, 1970; ISBN 978-87-571-0341-0.
- Potchter, O.; Cohen, P.; Lin, T.-P.; Matzarakis, A. Outdoor Human Thermal Perception in Various Climates: A Comprehensive Review of Approaches, Methods and Quantification. *Sci. Total Environ.* **2018**, *631–632*, 390–406. [CrossRef]
- Spagnolo, J.; de Dear, R. A Field Study of Thermal Comfort in Outdoor and Semi-Outdoor Environments in Subtropical Sydney Australia. *Build. Environ.* **2003**, *38*, 721–738. [CrossRef]
- Van Hoof, J.; Mazej, M.; Hensen, J.L.M. Thermal Comfort: Research and Practice. *Front. Biosci.* **2010**, *15*, 765–788. [CrossRef] [PubMed]
- Ahmadi Venhari, A.; Tenpierik, M.; Taleghani, M. The Role of Sky View Factor and Urban Street Greenery in Human Thermal Comfort and Heat Stress in a Desert Climate. *J. Arid Environ.* **2019**, *166*, 68–76. [CrossRef]
- Tian, Y.; Hong, B.; Zhang, Z.; Wu, S.; Yuan, T. Factors Influencing Resident and Tourist Outdoor Thermal Comfort: A Comparative Study in China's Cold Region. *Sci. Total Environ.* **2022**, *808*, 152079. [CrossRef] [PubMed]
- Darbani, E.S.; Rafieian, M.; Parapari, D.M.; Guldmann, J.-M. Urban Design Strategies for Summer and Winter Outdoor Thermal Comfort in Arid Regions: The Case of Historical, Contemporary and Modern Urban Areas in Mashhad, Iran. *Sustain. Cities Soc.* **2023**, *89*, 104339. [CrossRef]
- Lai, D.; Liu, W.; Gan, T.; Liu, K.; Chen, Q. A Review of Mitigating Strategies to Improve the Thermal Environment and Thermal Comfort in Urban Outdoor Spaces. *Sci. Total Environ.* **2019**, *661*, 337–353. [CrossRef]
- de Faria Peres, L.; de Lucena, A.J.; Rotunno Filho, O.C.; de Almeida França, J.R. The Urban Heat Island in Rio de Janeiro, Brazil, in the Last 30 Years Using Remote Sensing Data. *Int. J. Appl. Earth Obs. Geoinf.* **2018**, *64*, 104–116. [CrossRef]
- Chaves, M.E.D.; Picoli, M.C.A.; Sanches, I.D. Recent Applications of Landsat 8/OLI and Sentinel-2/MSI for Land Use and Land Cover Mapping: A Systematic Review. *Remote Sens.* **2020**, *12*, 3062. [CrossRef]
- He, X.; Miao, S.; Shen, S.; Li, J.; Zhang, B.; Zhang, Z.; Chen, X. Influence of Sky View Factor on Outdoor Thermal Environment and Physiological Equivalent Temperature. *Int. J. Biometeorol.* **2015**, *59*, 285–297. [CrossRef] [PubMed]
- Middel, A.; Huff, M.; Krayenhoff, E.S.; Udupa, A.; Schneider, F.A. PanoMRT: Panoramic Infrared Thermography to Model Human Thermal Exposure and Comfort. *Sci. Total Environ.* **2023**, *859*, 160301. [CrossRef]
- Kong, F.; Yan, W.; Zheng, G.; Yin, H.; Cavan, G.; Zhan, W.; Zhang, N.; Cheng, L. Retrieval of Three-Dimensional Tree Canopy and Shade Using Terrestrial Laser Scanning (TLS) Data to Analyze the Cooling Effect of Vegetation. *Agric. For. Meteorol.* **2016**, *217*, 22–34. [CrossRef]
- Li, X.; Ratti, C.; Seiferling, I. Mapping Urban Landscapes Along Streets Using Google Street View. In *Advances in Cartography and GIScience*; Peterson, M.P., Ed.; Springer International Publishing: Cham, Switzerland, 2017; pp. 341–356.
- Rodríguez Algeciras, J.A.; Gómez Consuegra, L.; Matzarakis, A. Spatial-Temporal Study on the Effects of Urban Street Configurations on Human Thermal Comfort in the World Heritage City of Camagüey-Cuba. *Build. Environ.* **2016**, *101*, 85–101. [CrossRef]

21. Sharmin, M.; Tjoelker, M.G.; Pfautsch, S.; Esperon-Rodriguez, M.; Rymer, P.D.; Power, S.A. Tree Crown Traits and Planting Context Contribute to Reducing Urban Heat. *Urban For. Urban Green.* **2023**, *83*, 127913. [[CrossRef](#)]
22. Châfer, M.; Tan, C.L.; Cureau, R.J.; Hien, W.N.; Pisello, A.L.; Cabeza, L.F. Mobile Measurements of Microclimatic Variables through the Central Area of Singapore: An Analysis from the Pedestrian Perspective. *Sustain. Cities Soc.* **2022**, *83*, 103986. [[CrossRef](#)]
23. Zhang, J.; Khoshbakht, M.; Liu, J.; Gou, Z.; Xiong, J.; Jiang, M. A Clustering Review of Vegetation-Indicating Parameters in Urban Thermal Environment Studies towards Various Factors. *J. Therm. Biol.* **2022**, *110*, 103340. [[CrossRef](#)]
24. Page, M.J.; McKenzie, J.E.; Bossuyt, P.M.; Boutron, I.; Hoffmann, T.C.; Mulrow, C.D.; Shamseer, L.; Tetzlaff, J.M.; Akl, E.A.; Brennan, S.E.; et al. The PRISMA 2020 Statement: An Updated Guideline for Reporting Systematic Reviews. *BMJ* **2021**, *372*, n71. [[CrossRef](#)] [[PubMed](#)]
25. Schneider, D.; Schwalbe, E.; Maas, H.-G. Validation of Geometric Models for Fisheye Lenses. *ISPRS J. Photogramm. Remote Sens.* **2009**, *64*, 259–266. [[CrossRef](#)]
26. Stankiewicz, O.; Lafruit, G.; Domański, M. Chapter 1—Multiview Video: Acquisition, Processing, Compression, and Virtual View Rendering. In *Academic Press Library in Signal Processing*; Chellappa, R., Theodoridis, S., Eds.; Academic Press: Cambridge, MA, USA, 2018; Volume 6, pp. 3–74, ISBN 978-0-12-811889-4.
27. Krüger, E. Impact of Site-Specific Morphology on Outdoor Thermal Perception: A Case-Study in a Subtropical Location. *Urban Clim.* **2017**, *21*, 123–135. [[CrossRef](#)]
28. Boiné, K.; Demers, C.M.H.; Potvin, A. Spatio-Temporal Promenades as Representations of Urban Atmospheres. *Sustain. Cities Soc.* **2018**, *42*, 674–687. [[CrossRef](#)]
29. Miao, C.; Yu, S.; Hu, Y.; Zhang, H.; He, X.; Chen, W. Review of Methods Used to Estimate the Sky View Factor in Urban Street Canyons. *Build. Environ.* **2020**, *168*, 106497. [[CrossRef](#)]
30. Gates, D.M.; Keegan, H.J.; Schleiter, J.C.; Weidner, V.R. Spectral Properties of Plants. *Appl. Opt.* **1965**, *4*, 11–20. [[CrossRef](#)]
31. Konarska, J.; Klingberg, J.; Lindberg, F. Applications of Dual-Wavelength Hemispherical Photography in Urban Climatology and Urban Forestry. *Urban For. Urban Green.* **2021**, *58*, 126964. [[CrossRef](#)]
32. Du, K.; Ning, J.; Yan, L. How Long Is the Sun Duration in a Street Canyon?—Analysis of the View Factors of Street Canyons. *Build. Environ.* **2020**, *172*, 106680. [[CrossRef](#)]
33. Li, Y.; Ouyang, W.; Yin, S.; Tan, Z.; Ren, C. Microclimate and Its Influencing Factors in Residential Public Spaces during Heat Waves: An Empirical Study in Hong Kong. *Build. Environ.* **2023**, *236*, 110225. [[CrossRef](#)]
34. Morakinyo, T.E.; Lau, K.K.-L.; Ren, C.; Ng, E. Performance of Hong Kong’s Common Trees Species for Outdoor Temperature Regulation, Thermal Comfort and Energy Saving. *Build. Environ.* **2018**, *137*, 157–170. [[CrossRef](#)]
35. Kong, L.; Lau, K.K.-L.; Yuan, C.; Chen, Y.; Xu, Y.; Ren, C.; Ng, E. Regulation of Outdoor Thermal Comfort by Trees in Hong Kong. *Sustain. Cities Soc.* **2017**, *31*, 12–25. [[CrossRef](#)]
36. Kong, H.; Choi, N.; Park, S. Thermal Environment Analysis of Landscape Parameters of an Urban Park in Summer—A Case Study in Suwon, Republic of Korea. *Urban For. Urban Green.* **2021**, *65*, 127377. [[CrossRef](#)]
37. Speak, A.F.; Salbitano, F. Summer Thermal Comfort of Pedestrians in Diverse Urban Settings: A Mobile Study. *Build. Environ.* **2022**, *208*, 108600. [[CrossRef](#)]
38. Öztürk, M.; Ağırtaş, L. Canopy Parameters for Tree and Shrub Species Compositions in Differently Intervened Land Uses of an Urban Park Landscape. *Build. Environ.* **2021**, *206*, 108340. [[CrossRef](#)]
39. Song, B. Comparison of Thermal Environments and Classification of Physical Environments Using Fisheye Images with Object-Based Classification. *Urban Clim.* **2023**, *49*, 101510. [[CrossRef](#)]
40. Acuña Paz y Miño, J.; Lawrence, C.; Beckers, B. Visual Metering of the Urban Radiative Environment through 4 π Imagery. *Infrared Phys. Technol.* **2020**, *110*, 103463. [[CrossRef](#)]
41. Lam, C.K.C.; Shooshtarian, S.; Kenawy, I. Assessment of Urban Physical Features on Summer Thermal Perceptions Using the Local Climate Zone Classification. *Build. Environ.* **2023**, *236*, 110265. [[CrossRef](#)]
42. Drach, P.; Krüger, E.L.; Emmanuel, R. Effects of Atmospheric Stability and Urban Morphology on Daytime Intra-Urban Temperature Variability for Glasgow, UK. *Sci. Total Environ.* **2018**, *627*, 782–791. [[CrossRef](#)]
43. Elsadek, M.; Liu, B.; Lian, Z.; Xie, J. The Influence of Urban Roadside Trees and Their Physical Environment on Stress Relief Measures: A Field Experiment in Shanghai. *Urban For. Urban Green.* **2019**, *42*, 51–60. [[CrossRef](#)]
44. Lamarca, C.; Qüense, J.; Henríquez, C. Thermal Comfort and Urban Canyons Morphology in Coastal Temperate Climate, Concepción, Chile. *Urban Clim.* **2018**, *23*, 159–172. [[CrossRef](#)]
45. Sun, S.; Xu, X.; Lao, Z.; Liu, W.; Li, Z.; Higuera García, E.; He, L.; Zhu, J. Evaluating the Impact of Urban Green Space and Landscape Design Parameters on Thermal Comfort in Hot Summer by Numerical Simulation. *Build. Environ.* **2017**, *123*, 277–288. [[CrossRef](#)]
46. Deng, X.; Nie, W.; Li, X.; Wu, J.; Yin, Z.; Han, J.; Pan, H.; Lam, C.K.C. Influence of Built Environment on Outdoor Thermal Comfort: A Comparative Study of New and Old Urban Blocks in Guangzhou. *Build. Environ.* **2023**, *234*, 110133. [[CrossRef](#)]

47. Canan, F.; Golasi, I.; Ciancio, V.; Coppi, M.; Salata, F. Outdoor Thermal Comfort Conditions during Summer in a Cold Semi-Arid Climate. A Transversal Field Survey in Central Anatolia (Turkey). *Build. Environ.* **2019**, *148*, 212–224. [CrossRef]
48. Kim, S.W.; Brown, R.D. Pedestrians' Behavior Based on Outdoor Thermal Comfort and Micro-Scale Thermal Environments, Austin, TX. *Sci. Total Environ.* **2022**, *808*, 152143. [CrossRef] [PubMed]
49. Kim, J.; Lee, D.-K.; Brown, R.D.; Kim, S.; Kim, J.-H.; Sung, S. The Effect of Extremely Low Sky View Factor on Land Surface Temperatures in Urban Residential Areas. *Sustain. Cities Soc.* **2022**, *80*, 103799. [CrossRef]
50. Alijani, S.; Pourahmad, A.; Hatami Nejad, H.; Ziari, K.; Sodoudi, S. A New Approach of Urban Livability in Tehran: Thermal Comfort as a Primitive Indicator. Case Study, District 22. *Urban Clim.* **2020**, *33*, 100656. [CrossRef]
51. Colter, K.R.; Middel, A.C.; Martin, C.A. Effects of Natural and Artificial Shade on Human Thermal Comfort in Residential Neighborhood Parks of Phoenix, Arizona, USA. *Urban For. Urban Green.* **2019**, *44*, 126429. [CrossRef]
52. Middel, A.; Krayenhoff, E.S. Micrometeorological Determinants of Pedestrian Thermal Exposure during Record-Breaking Heat in Tempe, Arizona: Introducing the MaRTy Observational Platform. *Sci. Total Environ.* **2019**, *687*, 137–151. [CrossRef] [PubMed]
53. Kim, E.J.; Kim, H. Walking-Based Mobile Measurement: Examining Its Reliability for Spatial Thermal Characteristics in Urban Environments. *Urban Clim.* **2024**, *58*, 102154. [CrossRef]
54. Díaz, G.M.; Negri, P.A.; Lencinas, J.D. Toward Making Canopy Hemispherical Photography Independent of Illumination Conditions: A Deep-Learning-Based Approach. *Agric. For. Meteorol.* **2021**, *296*, 108234. [CrossRef]
55. Díaz, G.M.; Lang, M.; Kaha, M. Simple Calibration of Fisheye Lenses for Hemispherical Photography of the Forest Canopy. *Agric. For. Meteorol.* **2024**, *352*, 110020. [CrossRef]
56. Jonckheere, I.; Fleck, S.; Nackaerts, K.; Muys, B.; Coppin, P.; Weiss, M.; Baret, F. Review of Methods for in Situ Leaf Area Index Determination: Part I. Theories, Sensors and Hemispherical Photography. *Agric. For. Meteorol.* **2004**, *121*, 19–35. [CrossRef]
57. LI-COR LAI-2200C Plant Canopy Analyzer. Available online: https://www.licor.cn/22_LAI-2200C.html (accessed on 5 May 2024).
58. Konarska, J.; Tarvainen, L.; Bäcklin, O.; Rantfors, M.; Uddling, J. Surface Paving More Important than Species in Determining the Physiology, Growth and Cooling Effects of Urban Trees. *Landsc. Urban Plan.* **2023**, *240*, 104872. [CrossRef]
59. Hwang, R.-L.; Weng, Y.-T.; Huang, K.-T. Considering Transient UTCI and Thermal Discomfort Footprint Simultaneously to Develop Dynamic Thermal Comfort Models for Pedestrians in a Hot-and-Humid Climate. *Build. Environ.* **2022**, *222*, 109410. [CrossRef]
60. Gillner, S.; Vogt, J.; Tharang, A.; Dettmann, S.; Roloff, A. Role of Street Trees in Mitigating Effects of Heat and Drought at Highly Sealed Urban Sites. *Landsc. Urban Plan.* **2015**, *143*, 33–42. [CrossRef]
61. Shi, Y.; Zhang, Y. Urban Morphological Indicators of Urban Heat and Moisture Islands under Various Sky Conditions in a Humid Subtropical Region. *Build. Environ.* **2022**, *214*, 108906. [CrossRef]
62. Ringland, J.; Bohm, M.; Baek, S.-R. Characterization of Food Cultivation along Roadside Transects with Google Street View Imagery and Deep Learning. *Comput. Electron. Agric.* **2019**, *158*, 36–50. [CrossRef]
63. Lu, Y.; Ferranti, E.J.S.; Chapman, L.; Pfrang, C. Assessing Urban Greenery by Harvesting Street View Data: A Review. *Urban For. Urban Green.* **2023**, *83*, 127917. [CrossRef]
64. Cheng, L.; Chu, S.; Zong, W.; Li, S.; Wu, J.; Li, M. Use of Tencent Street View Imagery for Visual Perception of Streets. *ISPRS Int. J. Geo-Inf.* **2017**, *6*, 265. [CrossRef]
65. Mahabir, R.; Schuchard, R.; Crooks, A.; Croitoru, A.; Stefanidis, A. Crowdsourcing Street View Imagery: A Comparison of Mapillary and OpenStreetCam. *ISPRS Int. J. Geo-Inf.* **2020**, *9*, 341. [CrossRef]
66. Egli, V.; Zinn, C.; Mackay, L.; Donnellan, N.; Villanueva, K.; Mavoa, S.; Exeter, D.J.; Vandevijvere, S.; Smith, M. Viewing Obesogenic Advertising in Children's Neighbourhoods Using Google Street View. *Geogr. Res.* **2019**, *57*, 84–97. [CrossRef]
67. Yan, G.; Hu, R.; Luo, J.; Weiss, M.; Jiang, H.; Mu, X.; Xie, D.; Zhang, W. Review of Indirect Optical Measurements of Leaf Area Index: Recent Advances, Challenges, and Perspectives. *Agric. For. Meteorol.* **2019**, *265*, 390–411. [CrossRef]
68. Hugin Hugin–Panorama Photo Stitcher. Available online: <https://hugin.sourceforge.io/> (accessed on 8 May 2024).
69. He, N.; Li, G. Urban Neighbourhood Environment Assessment Based on Street View Image Processing: A Review of Research Trends. *Environ. Chall.* **2021**, *4*, 100090. [CrossRef]
70. Wang, L.; Hou, C.; Zhang, Y.; He, J. Measuring Solar Radiation and Spatio-Temporal Distribution in Different Street Network Direction through Solar Trajectories and Street View Images. *Int. J. Appl. Earth Obs. Geoinf.* **2024**, *132*, 104058. [CrossRef]
71. Hu, C.; Jia, S.; Zhang, F.; Xiao, C.; Ruan, M.; Thrasher, J.; Li, X. UPDExplainer: An Interpretable Transformer-Based Framework for Urban Physical Disorder Detection Using Street View Imagery. *ISPRS J. Photogramm. Remote Sens.* **2023**, *204*, 209–222. [CrossRef]
72. Guo, H.; Aviv, D.; Loyola, M.; Teitelbaum, E.; Houchois, N.; Meggers, F. On the Understanding of the Mean Radiant Temperature within Both the Indoor and Outdoor Environment, a Critical Review. *Renew. Sustain. Energy Rev.* **2020**, *117*, 109207. [CrossRef]
73. Merchant, C.; Meggers, F.; Hou, M.; Aviv, D.; Schneider, F.A.; Middel, A. Resolving Radiant: Combining Spatially Resolved Longwave and Shortwave Measurements to Improve the Understanding of Radiant Heat Flux Reflections and Heterogeneity. *Front. Sustain. Cities* **2022**, *4*, 869743. [CrossRef]

74. Asawa, T.; Oshio, H.; Tanaka, K. Portable Recording System for Spherical Thermography and Its Application to Longwave Mean Radiant Temperature Estimation. *Build. Environ.* **2022**, *222*, 109412. [[CrossRef](#)]
75. Lim, K.; Treitz, P.; Wulder, M.; St-Onge, B.; Flood, M. LiDAR Remote Sensing of Forest Structure. *Prog. Phys. Geogr. Earth Environ.* **2003**, *27*, 88–106. [[CrossRef](#)]
76. Zheng, G.; Moskal, L.M. Computational-Geometry-Based Retrieval of Effective Leaf Area Index Using Terrestrial Laser Scanning. *IEEE Trans. Geosci. Remote Sens.* **2012**, *50*, 3958–3969. [[CrossRef](#)]
77. Xu, W.; Su, Z.; Feng, Z.; Xu, H.; Jiao, Y.; Yan, F. Comparison of Conventional Measurement and LiDAR-Based Measurement for Crown Structures. *Comput. Electron. Agric.* **2013**, *98*, 242–251. [[CrossRef](#)]
78. He, Y.; Yuan, C.; Ren, C.; Ng, E. Urban Ventilation Assessment with Improved Vertical Wind Profile in High-Density Cities—Comparisons between LiDAR and Conventional Methods. *J. Wind Eng. Ind. Aerodyn.* **2022**, *228*, 105116. [[CrossRef](#)]
79. Tian, B.; Loonen, R.C.G.M.; Hensen, J.L.M. Combining Point Cloud and Surface Methods for Modeling Partial Shading Impacts of Trees on Urban Solar Irradiance. *Energy Build.* **2023**, *298*, 113420. [[CrossRef](#)]
80. Gaitani, N.; Burud, I.; Thiis, T.; Santamouris, M. High-Resolution Spectral Mapping of Urban Thermal Properties with Unmanned Aerial Vehicles. *Build. Environ.* **2017**, *121*, 215–224. [[CrossRef](#)]
81. Song, B.; Park, K.; Kim, S.-H.; Park, G. Comparison of an Unmanned Aerial Vehicle Based Physical Environment with Thermal Properties from In-Situ Measurements: Campus of Changwon National University, South Korea. *Sustain. Cities Soc.* **2023**, *98*, 104836. [[CrossRef](#)]
82. Kim, S.-H.; Park, K.-H.; Lee, S.-A.; Song, B.-G. Analysis of Thermal Environment Characteristics by Spatial Type Using UAV and ENVI-Met. *J. Korean Assoc. Geogr. Inf. Stud.* **2022**, *25*, 28–43. [[CrossRef](#)]
83. Lyu, R.; Pang, J.; Tian, X.; Zhao, W.; Zhang, J. How to Optimize the 2D/3D Urban Thermal Environment: Insights Derived from UAV LiDAR/Multispectral Data and Multi-Source Remote Sensing Data. *Sustain. Cities Soc.* **2023**, *88*, 104287. [[CrossRef](#)]
84. Zheng, Z.; Sun, N.; Chen, H.; Yin, R.; Wang, Z.; Liu, W.; Wang, Y. Exploring the Association between Openness Scale of Campus Street Spaces, Street Greenery, Campus Walkability and Physical Activity of College Students. *J. Transp. Health* **2024**, *38*, 101897. [[CrossRef](#)]
85. Qi, Q.; Meng, Q.; Wang, J.; Ren, P. Developing an Optimized Method for the ‘Stop-and-Go’ Strategy in Mobile Measurements for Characterizing Outdoor Thermal Environments. *Sustain. Cities Soc.* **2021**, *69*, 102837. [[CrossRef](#)]
86. Liang, J.; Gong, J.; Sun, J.; Zhou, J.; Li, W.; Li, Y.; Liu, J.; Shen, S. Automatic Sky View Factor Estimation from Street View Photographs—A Big Data Approach. *Remote Sens.* **2017**, *9*, 411. [[CrossRef](#)]
87. Nouri, A.S.; Costa, J.P.; Matzarakis, A. Examining Default Urban-Aspect-Ratios and Sky-View-Factors to Identify Priorities for Thermal-Sensitive Public Space Design in Hot-Summer Mediterranean Climates: The Lisbon Case. *Build. Environ.* **2017**, *126*, 442–456. [[CrossRef](#)]
88. Mahmoud, H.; Ghanem, H.; Sodoudi, S. Urban Geometry as an Adaptation Strategy to Improve the Outdoor Thermal Performance in Hot Arid Regions: Aswan University as a Case Study. *Sustain. Cities Soc.* **2021**, *71*, 102965. [[CrossRef](#)]
89. Lindberg, F.; Holmer, B.; Thorsson, S. SOLWEIG 1.0—Modelling Spatial Variations of 3D Radiant Fluxes and Mean Radiant Temperature in Complex Urban Settings. *Int. J. Biometeorol.* **2008**, *52*, 697–713. [[CrossRef](#)] [[PubMed](#)]
90. Huang, K.-T.; Yang, S.-R.; Matzarakis, A.; Lin, T.-P. Identifying Outdoor Thermal Risk Areas and Evaluation of Future Thermal Comfort Concerning Shading Orientation in a Traditional Settlement. *Sci. Total Environ.* **2018**, *626*, 567–580. [[CrossRef](#)]
91. Nunzio, A.D. SkyViewAnalysis. Available online: <https://github.com/AntonelloDN/SkyViewAnalysis> (accessed on 8 May 2024).
92. Lam, C.K.C.; Lee, H.; Yang, S.-R.; Park, S. A Review on the Significance and Perspective of the Numerical Simulations of Outdoor Thermal Environment. *Sustain. Cities Soc.* **2021**, *71*, 102971. [[CrossRef](#)]
93. Fröhlich, D.; Gangwisch, M.; Matzarakis, A. Effect of Radiation and Wind on Thermal Comfort in Urban Environments—Application of the RayMan and SkyHelios Model. *Urban Clim.* **2019**, *27*, 1–7. [[CrossRef](#)]
94. Ma, X.; Fukuda, H.; Zhou, D.; Gao, W.; Wang, M. The Study on Outdoor Pedestrian Thermal Comfort in Blocks: A Case Study of the Dao He Old Block in Hot-Summer and Cold-Winter Area of Southern China. *Sol. Energy* **2019**, *179*, 210–225. [[CrossRef](#)]
95. Carrasco-Hernandez, R.; Smedley, A.R.D.; Webb, A.R. Using Urban Canyon Geometries Obtained from Google Street View for Atmospheric Studies: Potential Applications in the Calculation of Street Level Total Shortwave Irradiances. *Energy Build.* **2015**, *86*, 340–348. [[CrossRef](#)]
96. Li, X.; Ratti, C.; Seiferling, I. Quantifying the Shade Provision of Street Trees in Urban Landscape: A Case Study in Boston, USA, Using Google Street View. *Landsc. Urban Plan.* **2018**, *169*, 81–91. [[CrossRef](#)]
97. Soft Energy Photolux. Available online: <https://www.photolux-luminance.com/photolux> (accessed on 8 May 2024).
98. Forest Densimeters Spherical Densimeter. Available online: <https://www.forestdensimeter.com/about-the-densimeter> (accessed on 9 May 2024).
99. Ali, S.B.; Patnaik, S. Assessment of the Impact of Urban Tree Canopy on Microclimate in Bhopal: A Devised Low-Cost Traverse Methodology. *Urban Clim.* **2019**, *27*, 430–445. [[CrossRef](#)]

100. Forestry Tools Spherical Crown Densitometer–Convex Model A. Available online: <https://www.forestrytools.com.au/products/spherical-convex-densitometer> (accessed on 28 October 2024).
101. Chen, L.; Ng, E. Outdoor Thermal Comfort and Outdoor Activities: A Review of Research in the Past Decade. *Cities* **2012**, *29*, 118–125. [[CrossRef](#)]
102. Sharmin, T.; Steemers, K.; Matzarakis, A. Analysis of Microclimatic Diversity and Outdoor Thermal Comfort Perceptions in the Tropical Megacity Dhaka, Bangladesh. *Build. Environ.* **2015**, *94*, 734–750. [[CrossRef](#)]
103. Martinelli, L.; Matzarakis, A. Influence of Height/Width Proportions on the Thermal Comfort of Courtyard Typology for Italian Climate Zones. *Sustain. Cities Soc.* **2017**, *29*, 97–106. [[CrossRef](#)]
104. Yan, H.; Wu, F.; Nan, X.; Han, Q.; Shao, F.; Bao, Z. Influence of View Factors on Intra-Urban Air Temperature and Thermal Comfort Variability in a Temperate City. *Sci. Total Environ.* **2022**, *841*, 156720. [[CrossRef](#)] [[PubMed](#)]
105. Chatzidimitriou, A.; Yannas, S. Street Canyon Design and Improvement Potential for Urban Open Spaces; the Influence of Canyon Aspect Ratio and Orientation on Microclimate and Outdoor Comfort. *Sustain. Cities Soc.* **2017**, *33*, 85–101. [[CrossRef](#)]
106. Hsieh, C.-M.; Jan, F.-C.; Zhang, L. A Simplified Assessment of How Tree Allocation, Wind Environment, and Shading Affect Human Comfort. *Urban For. Urban Green.* **2016**, *18*, 126–137. [[CrossRef](#)]
107. Konijnendijk, C.C.; Ricard, R.M.; Kenney, A.; Randrup, T.B. Defining Urban Forestry—A Comparative Perspective of North America and Europe. *Urban For. Urban Green.* **2006**, *4*, 93–103. [[CrossRef](#)]
108. Liberalesso, T.; Oliveira Cruz, C.; Matos Silva, C.; Manso, M. Green Infrastructure and Public Policies: An International Review of Green Roofs and Green Walls Incentives. *Land Use Policy* **2020**, *96*, 104693. [[CrossRef](#)]
109. Georgi, J.N.; Dimitriou, D. The Contribution of Urban Green Spaces to the Improvement of Environment in Cities: Case Study of Chania, Greece. *Build. Environ.* **2010**, *45*, 1401–1414. [[CrossRef](#)]
110. Xiao, Q.; Fan, X.; Guo, Y.; Li, S.; He, W.; Deng, Y.; Xiao, Z.; Wang, P.; Wu, C. Tree Form Characteristics as Criteria for Tree Species Selection to Improve Pedestrian Thermal Comfort in Street Canyons: Case Study of a Humid Subtropical City. *Sustain. Cities Soc.* **2024**, *105*, 105339. [[CrossRef](#)]
111. Xu, M.; Hong, B.; Mi, J.; Yan, S. Outdoor Thermal Comfort in an Urban Park during Winter in Cold Regions of China. *Sustain. Cities Soc.* **2018**, *43*, 208–220. [[CrossRef](#)]
112. Han, D.; Xu, X.; Qiao, Z.; Wang, F.; Cai, H.; An, H.; Jia, K.; Liu, Y.; Sun, Z.; Wang, S.; et al. The Roles of Surrounding 2D/3D Landscapes in Park Cooling Effect: Analysis from Extreme Hot and Normal Weather Perspectives. *Build. Environ.* **2023**, *231*. [[CrossRef](#)]
113. Liu, Y.; Liu, T.; Jiang, L.; Shi, M.; Tan, X.; He, X.; Guo, J.; Shang, X. A Comparative Study of the Influences of Park Physical Factors on Summer Outdoor Thermal Environment, a Pilot Study of Mianyang, China. *Nat.-Based Solut.* **2023**, *4*, 100083. [[CrossRef](#)]
114. Liu, Z.; Brown, R.D.; Zheng, S.; Jiang, Y.; Zhao, L. An In-Depth Analysis of the Effect of Trees on Human Energy Fluxes. *Urban For. Urban Green.* **2020**, *50*, 126646. [[CrossRef](#)]
115. Yang, Y.; Zhou, D.; Gao, W.; Zhang, Z.; Chen, W.; Peng, W. Simulation on the Impacts of the Street Tree Pattern on Built Summer Thermal Comfort in Cold Region of China. *Sustain. Cities Soc.* **2018**, *37*, 563–580. [[CrossRef](#)]
116. Cheung, P.K.; Jim, C.Y. Comparing the Cooling Effects of a Tree and a Concrete Shelter Using PET and UTCI. *Build. Environ.* **2018**, *130*, 49–61. [[CrossRef](#)]
117. A Review of Studies and Modelling of Solar Radiation on Human Thermal Comfort in Outdoor Environment. *Build. Environ.* **2022**, *214*, 108891. [[CrossRef](#)]
118. Kántor, N.; Lin, T.-P.; Matzarakis, A. Daytime Relapse of the Mean Radiant Temperature Based on the Six-Directional Method under Unobstructed Solar Radiation. *Int. J. Biometeorol.* **2014**, *58*, 1615–1625. [[CrossRef](#)] [[PubMed](#)]
119. Du, J.; Sun, C.; Xiao, Q.; Chen, X.; Liu, J. Field Assessment of Winter Outdoor 3-D Radiant Environment and Its Impact on Thermal Comfort in a Severely Cold Region. *Sci. Total Environ.* **2020**, *709*, 136175. [[CrossRef](#)]
120. He, X.; Shao, L.; Tang, Y.; Wu, S. Improving Children’s Outdoor Thermal Comfort: A Field Study in China’s Severely Cold Regions. *Urban Clim.* **2023**, *51*, 101620. [[CrossRef](#)]
121. Chatzidimitriou, A.; Yannas, S. Microclimate Development in Open Urban Spaces: The Influence of Form and Materials. *Energy Build.* **2015**, *108*, 156–174. [[CrossRef](#)]
122. Kim, Y.J.; Brown, R.D. A Multilevel Approach for Assessing the Effects of Microclimatic Urban Design on Pedestrian Thermal Comfort: The High Line in New York. *Build. Environ.* **2021**, *205*, 108244. [[CrossRef](#)]
123. de Abreu-Harbach, L.V.; Labaki, L.C.; Matzarakis, A. Effect of Tree Planting Design and Tree Species on Human Thermal Comfort in the Tropics. *Landsc. Urban Plan.* **2015**, *138*, 99–109. [[CrossRef](#)]
124. Kim, Y.; Yu, S.; Li, D.; Gatson, S.N.; Brown, R.D. Linking Landscape Spatial Heterogeneity to Urban Heat Island and Outdoor Human Thermal Comfort in Tokyo: Application of the Outdoor Thermal Comfort Index. *Sustain. Cities Soc.* **2022**, *87*, 104262. [[CrossRef](#)]
125. Zhang, T.; Su, M.; Hong, B.; Wang, C.; Li, K. Interaction of Emotional Regulation and Outdoor Thermal Perception: A Pilot Study in a Cold Region of China. *Build. Environ.* **2021**, *198*, 107870. [[CrossRef](#)]

126. Niu, J.; Xiong, J.; Qin, H.; Hu, J.; Deng, J.; Han, G.; Yan, J. Influence of Thermal Comfort of Green Spaces on Physical Activity: Empirical Study in an Urban Park in Chongqing, China. *Build. Environ.* **2022**, *219*, 109168. [[CrossRef](#)]
127. Rahman, M.A.; Hartmann, C.; Moser-Reischl, A.; von Strachwitz, M.F.; Paeth, H.; Pretzsch, H.; Pauleit, S.; Rötzer, T. Tree Cooling Effects and Human Thermal Comfort under Contrasting Species and Sites. *Agric. For. Meteorol.* **2020**, *287*, 107947. [[CrossRef](#)]
128. Castaldo, V.L.; Pisello, A.L.; Pigliautile, I.; Piselli, C.; Cotana, F. Microclimate and Air Quality Investigation in Historic Hilly Urban Areas: Experimental and Numerical Investigation in Central Italy. *Sustain. Cities Soc.* **2017**, *33*, 27–44. [[CrossRef](#)]
129. Molenaar, R.E.; Heusinkveld, B.G.; Steeneveld, G.J. Projection of Rural and Urban Human Thermal Comfort in The Netherlands for 2050. *Int. J. Climatol.* **2016**, *36*, 1708–1723. [[CrossRef](#)]
130. Chen, L.; Zhang, Y.; Han, J.; Li, X. An Investigation of the Influence of Ground Surface Properties and Shading on Outdoor Thermal Comfort in a High-Altitude Residential Area. *Front. Archit. Res.* **2021**, *10*, 432–446. [[CrossRef](#)]
131. Liu, Y.; Zhang, M.; Li, Q.; Zhang, T.; Yang, L.; Liu, J. Investigation on the Distribution Patterns and Predictive Model of Solar Radiation in Urban Street Canyons with Panorama Images. *Sustain. Cities Soc.* **2021**, *75*, 103275. [[CrossRef](#)]
132. Kim, M.; Lee, K.; Cho, G.-H. Temporal and Spatial Variability of Urban Heat Island by Geographical Location: A Case Study of Ulsan, Korea. *Build. Environ.* **2017**, *126*, 471–482. [[CrossRef](#)]
133. Motazedian, A.; Coutts, A.M.; Tapper, N.J. The Microclimatic Interaction of a Small Urban Park in Central Melbourne with Its Surrounding Urban Environment during Heat Events. *Urban For. Urban Green.* **2020**, *52*, 126688. [[CrossRef](#)]
134. Tan, Z.; Lau, K.K.-L.; Ng, E. Planning Strategies for Roadside Tree Planting and Outdoor Comfort Enhancement in Subtropical High-Density Urban Areas. *Build. Environ.* **2017**, *120*, 93–109. [[CrossRef](#)]
135. Lam, C.K.C.; Hang, J. Solar Radiation Intensity and Outdoor Thermal Comfort in Royal Botanic Garden Melbourne during Heatwave Conditions. *Procedia Eng.* **2017**, *205*, 3456–3462. [[CrossRef](#)]
136. Cheung, P.K.; Fung, C.K.W.; Jim, C.Y. Seasonal and Meteorological Effects on the Cooling Magnitude of Trees in Subtropical Climate. *Build. Environ.* **2020**, *177*, 106911. [[CrossRef](#)]
137. Zhang, J.; Guo, W.; Cheng, B.; Jiang, L.; Xu, S. A Review of the Impacts of Climate Factors on Humans' Outdoor Thermal Perceptions. *J. Therm. Biol.* **2022**, *107*, 103272. [[CrossRef](#)]
138. Deevi, B.; Chundeli, F.A. Quantitative Outdoor Thermal Comfort Assessment of Street: A Case in a Warm and Humid Climate of India. *Urban Clim.* **2020**, *34*, 100718. [[CrossRef](#)]
139. Song, G.-S.; Jeong, M.-A. Morphology of Pedestrian Roads and Thermal Responses during Summer, in the Urban Area of Bucheon City, Korea. *Int. J. Biometeorol.* **2016**, *60*, 999–1014. [[CrossRef](#)]
140. Xue, F.; Gou, Z.; Lau, S.S.Y. Green Open Space in High-Dense Asian Cities: Site Configurations, Microclimates and Users' Perceptions. *Sustain. Cities Soc.* **2017**, *34*, 114–125. [[CrossRef](#)]
141. Zheng, S.; Guldmann, J.-M.; Liu, Z.; Zhao, L. Influence of Trees on the Outdoor Thermal Environment in Subtropical Areas: An Experimental Study in Guangzhou, China. *Sustain. Cities Soc.* **2018**, *42*, 482–497. [[CrossRef](#)]
142. Chen, X.; Zhao, P.; Hu, Y.; Ouyang, L.; Zhu, L.; Ni, G. Canopy Transpiration and Its Cooling Effect of Three Urban Tree Species in a Subtropical City- Guangzhou, China. *Urban For. Urban Green.* **2019**, *43*, 126368. [[CrossRef](#)]
143. Chen, K.; Tian, M.; Zhang, J.; Xu, X.; Yuan, L. Evaluating the Seasonal Effects of Building Form and Street View Indicators on Street-Level Land Surface Temperature Using Random Forest Regression. *Build. Environ.* **2023**, *245*, 110884. [[CrossRef](#)]
144. Liu, Z.; Li, J.; Xi, T. A Review of Thermal Comfort Evaluation and Improvement in Urban Outdoor Spaces. *Buildings* **2023**, *13*, 3050. [[CrossRef](#)]
145. Gong, F.-Y.; Zeng, Z.-C.; Zhang, F.; Li, X.; Ng, E.; Norford, L.K. Mapping Sky, Tree, and Building View Factors of Street Canyons in a High-Density Urban Environment. *Build. Environ.* **2018**, *134*, 155–167. [[CrossRef](#)]
146. Zeng, L.; Lu, J.; Li, W.; Li, Y. A Fast Approach for Large-Scale Sky View Factor Estimation Using Street View Images. *Build. Environ.* **2018**, *135*, 74–84. [[CrossRef](#)]
147. Xia, Y.; Yabuki, N.; Fukuda, T. Sky View Factor Estimation from Street View Images Based on Semantic Segmentation. *Urban Clim.* **2021**, *40*, 100999. [[CrossRef](#)]
148. Zhong, X.; Zhao, L.; Ren, P.; Zhang, X.; Wang, J. A Physics-Guided Automated Machine Learning Approach for Obtaining Surface Radiometric Temperatures on Sunny Days Based on UAV-Derived Images. *Comput. Environ. Urban Syst.* **2024**, *113*, 102175. [[CrossRef](#)]
149. Witzmann, S.; Gollob, C.; Kraßnitzer, R.; Ritter, T.; Tockner, A.; Schume, H.; Nothdurft, A. Modeling of Solar Radiation and Sub-Canopy Light Regime on Forest Inventory Plots of Mixed Conifer and Deciduous Temperate Forests Using Point Clouds from Personal Laser Scanning. *For. Ecol. Manag.* **2024**, *569*, 122166. [[CrossRef](#)]
150. Cheung, P.K.; Jim, C.Y. Differential Cooling Effects of Landscape Parameters in Humid-Subtropical Urban Parks. *Landsc. Urban Plan.* **2019**, *192*, 103651. [[CrossRef](#)]
151. Steyn, D.G. The Calculation of View Factors from Fisheye-lens Photographs: Research Note. *Atmos.-Ocean* **1980**, *18*, 254–258. [[CrossRef](#)]

152. Chapman, L.; Thornes, J.E.; Bradley, A.V. Rapid Determination of Canyon Geometry Parameters for Use in Surface Radiation Budgets. *Theor. Appl. Climatol.* **2001**, *69*, 81–89. [[CrossRef](#)]
153. Nikolopoulou, M.; Steemers, K. Thermal Comfort and Psychological Adaptation as a Guide for Designing Urban Spaces. *Energy Build.* **2003**, *35*, 95–101. [[CrossRef](#)]
154. Kruger, E.L.; Drach, P. Identifying Potential Effects from Anthropometric Variables on Outdoor Thermal Comfort. *Build. Environ.* **2017**, *117*, 230–237. [[CrossRef](#)]
155. Xu, M.; Hong, B.; Jiang, R.; An, L.; Zhang, T. Outdoor Thermal Comfort of Shaded Spaces in an Urban Park in the Cold Region of China. *Build. Environ.* **2019**, *155*, 408–420. [[CrossRef](#)]
156. Kumar, P.; Sharma, A. Study on Importance, Procedure, and Scope of Outdoor Thermal Comfort—A Review. *Sustain. Cities Soc.* **2020**, *61*, 102297. [[CrossRef](#)]
157. Chan, S.Y.; Chau, C.K. A Study of Subtropical Park Thermal Comfort and Its Influential Factors during Summer. *Sustain. Cities Soc.* **2021**, *64*, 102512. [[CrossRef](#)]
158. Chokhachian, A.; Ka-Lun Lau, K.; Perini, K.; Auer, T. Sensing Transient Outdoor Comfort: A Georeferenced Method to Monitor and Map Microclimate. *J. Build. Eng.* **2018**, *20*, 94–104. [[CrossRef](#)]
159. de Dear, R. Revisiting an Old Hypothesis of Human Thermal Perception: Alliesthesia. *Build. Res. Inf.* **2011**, *39*, 108–117. [[CrossRef](#)]

Disclaimer/Publisher’s Note: The statements, opinions and data contained in all publications are solely those of the individual author(s) and contributor(s) and not of MDPI and/or the editor(s). MDPI and/or the editor(s) disclaim responsibility for any injury to people or property resulting from any ideas, methods, instructions or products referred to in the content.